

REGULATION OF THE BMI1 AND RET PROTO-ONCOGENES BY THE DLX2
TRANSCRIPTION FACTOR IN THE DEVELOPING GASTRO-INTESTINAL TRACT

by

Hunter Donald McColl

A thesis submitted in partial fulfillment of the requirements for the degree of

Master of Science

Medical Sciences - Medical Genetics
University of Alberta

© Hunter Donald McColl, 2017

Abstract:

The *Dlx1/Dlx2* double knockout (DKO) mouse dies at P0 with a cleft palate and a distended abdomen. Within the intestinal crypts of Leiberkuhn a stable, non-dividing stem cell group is marked by the oncogene *BMI1*. Unpublished data from the Eisenstat laboratory demonstrates co-expression of *BMI1* and the homeobox transcription factor *DLX2* in the intestinal crypts and also suggests a role for *DLX2* in the regulation of expression of the *Ret* proto-oncogene. *Ret* is responsible for enteric nervous system (ENS) development. Over-expression of *RET* induces Multiple Endocrine Neoplasia syndrome type cancers whereas *RET* loss-of-function is associated with Hirschsprung's Disease (HD) with partial or complete loss of intestinal innervation. We investigated the potential regulatory effect of *DLX2* on *Bmi1* and *Ret*. Our **hypothesis** was that *DLX2* suppresses *Bmi1* while promoting *Ret* expression through direct binding of the gene targets' promoters during intestinal and ENS development.

Methods:

Chromatin Immunoprecipitation (ChIP) assays using a polyclonal *DLX2* antibody and embryonic intestinal tissues studied candidate *in vivo* interactions between *DLX2* and target promoter regions of genomic DNA. Electrophoretic mobility shift assays (EMSAs) and site directed mutagenesis of *DLX2* binding sites was used to determine if there was direct binding by *DLX2* of the *Bmi1/ Ret* regulatory regions identified by ChIP *in vitro*. Reporter gene assays were applied to assess the effect of *Dlx2* co-expression on *Bmi1/ Ret* expression *in vitro*. Quantitative PCR analysis of the embryonic gastrointestinal tract demonstrated the *in vivo* effect of loss of *Dlx1/Dlx2* expression on *Ret* and *Bmi1* expression when comparing wild-type to *Dlx1/Dlx2* DKO mouse tissues.

Results:

DLX2 interaction with specific regions of the *Bmi1* and *Ret*'s promoters *in vivo* was demonstrated using ChIP. The potential for specific binding of *DLX2* to only a subset of the promoters identified by ChIP assays *in vitro* was demonstrated by EMSA assay. The *in vitro* regulatory effects of *DLX2* on the expression of these genes were revealed through luciferase gene reporter assays: *Ret* expression was repressed whereas *Bmi1* expression was activated. *In*

in vivo analysis shows a significant change in *ret* expression in the *Dlx1/Dlx2* DKO when measured by qPCR. *Ret* expression was decreased in the small intestine and increased in the large intestine at E13 in the DKO. However, *Bmi1* shows no change in intestinal expression at E18 with the loss of *Dlx1/Dlx2* gene function.

Conclusion:

Occupancy of the *Bmi1* and *Ret* promoters by DLX2 *in vivo* occurs at specific time points, while EMSAs demonstrate direct binding of DLX2 to specific promoter regions *in vitro*. While reporter gene assays show the ability of DLX2 to repress *ret* expression *in vitro*, *in vivo* this regulation may be influenced by proximal/distal patterning which may also underlie the severity of the various phenotypes of HD. While DLX2 shows *in vitro* regulatory potential over *Bmi1* expression, *in vivo* assays did not support a regulatory interaction during embryonic development. Ongoing expression studies of cell-type specific markers for epithelial and ganglion cell markers in the intestine and ENS in the *Dlx1/Dlx2* DKO mouse as well as in human HD biopsies will further explore the biological significance of DLX2 on intestinal and ENS development.

Acknowledgements:

My time at the University of Alberta has been long, winding and exhausting. However, at no one point was I ever on my own on the path that led to this moment. I have been helped and at times carried by those willing to let me into their lives and support me.

Firstly, I thank the Hair Massacure Fund and WCHRI (Women's and Children Health Research Institute) for funding this project, enabling me to perform my research and follow my passion for genetics.

Secondly I thank my supervisor and mentor Dr. David Eisenstat. You took me into your lab on a risk, having just moved from Winnipeg with no real guarantee of what kind of student you would be getting. Without your openness to overlook flaws that were on paper and vouching for my aptitude I would never have made it to this point. Thank you for your constant support and endorsements, your guidance has helped me further along than I could have dreamed the first time I met with you in your office.

To my Committee members Dr Consolato Sergi and Dr Rachel Wevrick, thank you for your support, your questions and for pushing me to always be improving and learning.

My lab members have become like family, and none of this could have been finished without the help you all gave me. Sarah and Maryam, we started in the lab together at the same time and have shared so much through the years. Thank you for the all laughter we shared in lab and for helping me to become more social outside of it; I know you will both finish strong and go far. Allison, we had less time together in lab but it feels like you have always been there, thank you for being willing to listen to me complain, and ask questions about dumb things and always having a great outlook on where science will take us.

A special thanks goes to Jamie Zagozewski. You are as much a mentor as you are a friend; you have put up with so many questions and have helped me in so many ways with my project that I truly do not believe I could have done it without you in being there. You will go on to do great things as you enter a new phase of your life. Keep you passion for science alight as you go on to your next big adventure.

To my family I say thank you for being there to support me and distract me as needed. You will always be part of any of my accomplishments, keeping me grounded and humble.

To the other members of Medical Genetics, graduate students and professors alike: that I have been able to spend time with such fun, inspiring people is a great gift, and I hope to stay in touch with as many of you as I can.

Outside of the Department there are some groups I would like to thank. To my amazing 420s who I love with all my heart – I got out first, therefore I win! Thank you guys for being there when I needed someone to complain to or to make me laugh. I am looking forward to seeing what the future holds for us. To my rock climbing friends I thank you for keeping me safe when I blow off steam at the wall, and being there to catch me when I fall (literally). To those special people in my life who never fail to brighten my day (you know who you are) thank you for supporting me in all aspects, especially through the stress of the past few months. I am looking forward to finding a new normal with you all, hopefully it means more time with each other.

This is the culmination of my time as a post-secondary student, and it is bittersweet to see it come to a close. As much as I have been heard talking about my eagerness to finish, I am also filled with trepidation as I transition from one stage of my life to another. I know, however, that I have amazing people in my life who will help make this change palatable. Thank you all.

Table of Contents:

Chapter 1: Introduction.....	1
1.1 <i>Embryonic Development of the Gastro-Intestinal Tract</i>	2
1.2 <i>The Intestinal Wall</i>	4
1.3 <i>The Intestinal Epithelium</i>	7
1.4 <i>Intestinal Stem Cell Niche</i>	11
1.5 <i>Bmi1 and the Polycomb Repressive Complex</i>	12
1.6 <i>Intrinsic innervation of the GIT by the neural crest</i>	13
1.7 <i>The ret proto-oncogene</i>	17
1.8 <i>Hirschsprung Disorder</i>	21
1.9 <i>Homeobox genes</i>	25
Chapter 2: Hypothesis and Research Aims.....	29
2.1 <i>Hypotheses</i>	30
2.2 <i>Aim 1</i>	30
2.2 <i>Aim 2</i>	30
2.2 <i>Aim 3</i>	30
Chapter 3: Material and Methods.....	32
3.1 <i>Animal and Tissues Collected</i>	33
3.2 <i>Tissue Preparation, Fixation & Sectioning</i>	33
3.3 <i>Chromatin Immunoprecipitation</i>	34
3.4 <i>Molecular Cloning</i>	36

3.5 Immunofluorescence Analyses	37
3.6 Immunohistochemistry Analysis	37
3.8 Electrophoretic Mobility Shift Assay	39
3.9 Luciferase Gene Reporter Assay	40
3.10 Quantitative Reverse Transcription Polymerase Chain Reaction	40
3.11 Site Directed Mutagenesis	41
Chapter 4: <i>Ret</i> proto-oncogene regulation by <i>Dlx2</i> : Results	46
4.1 <i>DLX2</i> and <i>RET</i> co-expression is observed in a subset of enteric ganglia within ganglionic positive regions of human Hirschsprung's patient intestinal samples	47
4.2 The <i>Ret</i> upstream regulatory region contains multiple homeodomain binding regions ..	50
4.3 <i>DLX2</i> occupies the <i>Ret</i> promoter in vivo in the mouse model	53
4.4 <i>DLX2</i> directly binds to the <i>Ret</i> regulatory region in vitro	56
4.5 <i>Dlx2</i> co-expression significantly inhibits <i>Ret</i> reporter gene expression in vitro	59
4.6 <i>Dlx1/Dlx2</i> has a significant regulatory effect over <i>Ret</i> in vivo in the developing small and large intestines	62
Chapter 5: <i>Bmi1</i> regulation by <i>DLX2</i> : Results	67
5.1 <i>DLX2</i> and <i>Bmi1</i> co-expression is observed in a subset of cells within the adult mouse intestinal Crypts of Lieberkuhn	68
5.2 The <i>Bmi1</i> upstream regulatory region contains many homeodomain binding regions ...	71
5.3 <i>DLX2</i> occupies the <i>Bmi1</i> promoter in vivo in the mouse model	74
5.4 <i>DLX2</i> directly binds to <i>Bmi1</i> regulatory regions in vitro	77

5.5 <i>Dlx2</i> co-expression significantly activates <i>Bmi1</i> Regions 1 & 3 <i>in vitro</i>	82
5.6 Loss of <i>DLX2</i> appears to have no effect on <i>Bmi1</i> expression in the developing mouse intestine <i>in vivo</i> at E18.5 in preliminary experiments.....	85
Chapter 6: Discussion.....	88
6.1 <i>Dlx2</i> and <i>Ret</i> expression in the developing intestinal tract.....	89
6.2 <i>DLX2</i> directly binds the <i>RET</i> 5' regulatory region during intestinal development.....	90
6.3 Loss of <i>Dlx1/2</i> gene function activates <i>Ret</i> in the developing small intestine while repressing it in the large intestine at E13.5.....	91
6.4 <i>Dlx2</i> directly binds the <i>Bmi1</i> regulatory region in the developing intestinal tract.....	93
6.5 <i>DLX2</i> Transcriptionally activates <i>Bmi1</i> regions <i>in vitro</i>	94
Chapter 7: Conclusions and Future Directions.....	95
Literature Cited.....	98

Permissions:

Figures requiring permission for use in this thesis were figures 2, 3, and 4. Permission for the inclusion of these figures has been granted, with reference numbers included in the figure legends. Figure 1 does not require any permissions as of 2017 in accordance with the creative common licence. Permission is not required from the Nature Publishing Group for Figure 5 as it is the author's own work.

List of Tables:

Table 1. Primer sets for amplification of ChIP products of <i>Ret</i> and <i>Bmi1</i> regulatory regions.....	37-38
Table 2. Primer sets for cloning of ChIP positive regions into pGL3 vector. Restriction sites are highlighted.....	38
Table 3. Antibodies used in immunohistochemical and immunofluorescence analyses of GI tissues.....	39
Table 4. Primer sets used for site directed mutagenesis of <i>Bmi1</i> Region 1, altered nucleotides are highlighted.....	40
Table 5. Primers designed for use in RT-PCR experiments.....	40

List of Figures:

Figure 1. Representation of the layers of the intestinal wall.....	4
Figure 2. The intestinal stem cell niche of the Crypts of Lieberkuhn in the small and large intestines.....	8
Figure 3. Differentiation of Neural Crest Cells into enteric neuronal and glial subtypes.....	14
Figure 4. Cell signalling cascade involved with the GDNF RET signalling pathways.....	16
Figure 5. Mutations of Ret and their effects on patient presentation of Hirschprung's Disease.....	21
Figure 6. Dlx1/2 Double knockout mouse P0 pup.....	24
Figure 7. Spatial expression patterns of DLX2 and RET in human HD patient intestinal epithelium and ganglionic intestinal plexus.....	42
Figure 8. Schematic of 4kb regulatory regions upstream of target gene transcriptional start sites....	45
Figure 9. DLX2 occupies specific regulatory regions of <i>ret in vivo</i> in the developing mouse gastrointestinal tract.....	48

Figure 10. DLX2 directly interacts with <i>Ret</i> regulatory region 3 <i>in vitro</i>	51
Figure 11. DLX2 restricts <i>Ret</i> R3 expression <i>in vitro</i>	54
Figure 12. Quantitative real time PCR analysis of the effect that loss of <i>Dlx1/2</i> gene function has on <i>Ret</i> expression <i>in vivo</i>	57
Figure 13. Quantitative PCR of E13 proximal (small intestine) and distal (colon) GIT show significant differences in expression in the absence of <i>Dlx1/2</i> gene function.....	59
Figure 14. DLX2 is expressed in the cells of the intestinal Crypts of Lieberkuhn and colocalizes with BMI1 in the stem cell populations.....	62
Figure 15. Schematic of 4kb regulatory region upstream of <i>Bmi1</i> transcriptional start site.....	65
Figure 16. DLX2 occupies specific regulatory regions of <i>Bmi1</i> <i>in vivo</i> in the developing mouse gastrointestinal tract.....	68
Figure 17. DLX2 directly interacts with <i>Bmi1</i> regulatory regions 1, 3, and 5 <i>in vitro</i>	71
Figure 18. Site directed mutagenesis abolishment of distinct binding sites can determine critical homeodomain motifs for DLX2 binding <i>in vitro</i>	73
Figure 19. <i>Dlx2</i> co-expression activates <i>Bmi1</i> R3 expression <i>in vitro</i>	76
Figure 20. Preliminary qPCR of <i>Bmi1</i> expression shows no significant difference upon the loss of <i>Dlx1/2</i> gene function.....	79

Abbreviations:

APS.....	Ammonium Persulfate
<i>Bmi1</i>	B lymphoma Mo-MLV insertion region 1 homolog
<i>Bmi1</i>	<i>Bmi1</i> gene (mouse)
BSA.....	Bovine serum albumin
C.....	Celsius
CBC.....	Crypt Basal Cells
<i>Cbx</i>	Chromobox homologue
ChIP.....	Chromatin immunoprecipitation assays
CNS.....	Central nervous system

CPM	Counts per minute
<i>Dlx</i>	distal-less homeobox gene (mouse gene is in italics)
Dlx1/2DKO	Dlx1/Dlx2 double knockout
DLX2	Dlx2 homeobox protein (capital letters)
E13	Embryonic day 13
E18	Embryonic day 18
EDNRB	Endothelin Receptor B
EDTA	Ethylenediaminetetraacetic acid
EMSA	electrophoretic mobility shift assays
ENCC	Enteric Neural Crest-Derived Cells
ENS	Enteric Nervous System
FFPE	Formalin-fixed paraffin embedded
GDNF	Glial derived neurotrophic factors
GDNF α 1	Glial Derived Neurotrophic Factor α 1
GIT	Gastro-intestinal tract
H2AK119ub1	Monoubiquitination of histone 2A Lysine 119
H3K4M3	Histone 3 lysine 4 trimethylation
H3K27Ac	Histone 3 lysine 27 acetylation
H3K27Me3	Trimethylation of lysine 27 on histone 3
HD	Hirschsprung's Disease
IF	Immunofluorescence
IGGs	Immunoglobulin Gs
IHC	Immunohistochemistry
Hox	Homeobox
ISCs	Intestinal stem cells
ITTs	indwelling transanal tubes
KDM2b	Lysine Demethylase 2B
KO	Knockout

LB.....	Lysogeny Broth
Lgr5.....	Leucine-rich repeat-containing G-protein coupled receptor 5
MEN2.....	multiple endocrine neoplasia type 2
MTC.....	medullary carcinoma of the thyroid
NCC.....	Neural crest cells
NCDC.....	Neural Crest Derived Cells
OCT.....	Optimal Cutting Temperature Compound
P0.....	Postnatal day 0
P ³² -dNTP.....	Phosphorous 32 isotope dNTP
PBS.....	Phosphate Buffer Saline
PcG.....	Polycomb group gene
PFA.....	Paraformaldehyde
PIC.....	Protease Inhibitor Cocktail
PRC1.....	Polycomb Repressive Complex 1
PRC2.....	Polycomb Repressive Complex 2
pY1062.....	phosphorylation at tyrosine 1062
q-ISCs.....	Quiescent intestinal stem cells
q-rtPCR.....	Quantitative reverse transcription PCR
Ret.....	Rearranged during transcription
<i>Ret</i>	Ret gene (mouse)
<i>RET</i>	RET gene (human)
RT-PCR.....	Reverse transcription PCR
RYBP.....	RING1 binding protein
SDM.....	Site directed mutagenesis
SRY.....	Sex determining factor Y
TA.....	Transit amplifying
TBE.....	Tris/Borate/EDTA buffer
TE.....	Tris-EDTA buffer

TEMED.....Tetramethylethylenediamine

WT..... Wild type

Chapter 1: Introduction

1.1 *Embryonic Development of the Gastro-Intestinal Tract*

The gastro-intestinal tract (GIT) is a large organ system consisting of the esophagus, stomach and intestines (Montgomery, Mulberg et al. 1999). It arises from the endoderm germ layer (Zorn and Wells 2009) following gastrulation in the Carnegie Stage 7 (about 3 weeks post fertilization) of human development, forming a bi-layered primitive gut tube due to cranial and caudal folding (Solomon, Berg et al. 2002). Once gastrulation establishes the three primary layers (ectoderm, endoderm, and mesoderm), the endoderm folds at both the anterior and posterior ends. This creates pockets of endoderm with an opening exposed to the yolk sac that will form the primitive tube. As the endoderm continues to fold inward, expanding along the cranial-caudal axis the opening to the yolk sac draws tighter, forming the yolk stalk and the distinct structures of the primitive tube (the foregut, midgut and hindgut), which become distinguishable at Carnegie stage 9 (Solomon, Berg et al. 2002) and develop in tandem with each other.

Both the esophagus and stomach develop from the foregut, which generates the most anterior structures of the GIT, as well as the upper duodenum, part of the fully developed small intestine. The early esophagus is formed as the foregut develops two ridges known as tracheoesophageal folds, which divide the foregut tube into trachea (ventral) and esophagus (dorsal) (Montgomery, Mulberg et al. (1999). The esophagus remains short until the 10th Carnegie stage, when it begins elongating to keep up with the lengthening of the embryo. The stomach begins forming during stage 10, shortly after the esophagus is distinguishable. The caudal foregut begins dilating and undergoing a series of rotations along the longitudinal axis and the transverse axis reorienting the stomach and allowing proper expansion and movement of the pylorus and esophageal openings (Sadler and Langman 2012). The most distal segment of the foregut becomes the anterior segment of the developing duodenum, a structure of the small intestine. The duodenum is divided into four segments, two of which are derived from the foregut and two from the midgut. Beginning at the pylorus, the foregut gives rise to the superior and descending segments of the duodenum; these segments are the most proximal components of the small intestine. Joining with the foregut at the inferior duodenal flexure, the midgut derived inferior and ascending segments form a complete duodenum with four segments.

The midgut develops concurrently with the other two GIT developmental regions, contributing most to the development of the small and large intestines. The posterior duodenum, jejunum, and

ileum (making up the small intestine), as well as the cecum and proximal two thirds of the large intestine are all derived from this structure (Solomon, Berg et al. 2002). By stage 10 the midgut is communicating with the yolk sac, and as development progresses midgut expansion helps to create the vitelline duct (Pansky 1982). Generation of the intestinal structures by the midgut begins at stage 22 when the elongated midgut herniates into the somatic coelom, which provides more room for the midgut to continue growing. The proximal side of the loop ultimately develops into the distal duodenum, jejunum and the proximal ileum. The distal loop rotates slightly clockwise, setting up the midgut for later rotations that coordinate intestinal positioning. At the time of this initial rotation the proximal loop expands into coils, increasing its surface area and setting itself up for differentiation into the small intestinal structures. A small bulge develops into the distal loop, which will become the cecum (Montgomery, Mulberg et al. 1999). As this occurs the abdominal cavity of the embryo grows to accommodate the midgut. By week 10 of development the proximal loop returns first, crossing beneath the distal loop and moves over top of the hindgut. Once the proximal loop is re-established within the fetal abdominal cavity, the distal loop re-enters. As it returns to the body cavity the distal loop rotates further clockwise, setting the stage for the lower small intestine and the large intestine as it is now in place to form the ascending and transverse colons that pass over the distal duodenum (Montgomery, Mulberg et al. 1999).

The final structures of the GIT develop from the hindgut, the most distal structure of the primitive tube, ending at the cloacal pouch. Its development completes the transverse, descending and sigmoid colons of the large intestine, as well as the cecum and rectum. By stage 10 the hindgut is still a simple tube ending in the cloaca, with no distinct structures (Montgomery, Mulberg et al. 1999). Development progresses as the mesenchyme derived urorectal septum descends through the cloaca, lengthening the hindgut as it travels to fuse with the cloacal membrane by Stage 20. This fusion separates the membrane into the urogenital and anal membranes, creating a distinct rectal canal. By Stage 23 the anal membrane ruptures via apoptosis creating an opening from the anal canal to the outside environment. This opening is then closed by an epithelial plug until later in fetal development (de Vries and Friedland 1974). The development of the colon's epithelial structures occurs concurrently with the expansions and rotations of the midgut.

Intestinal development continues throughout fetal development and postnatal stages, completing necessary events such as colonization of the GI tract with microbiota necessary for digestion, differentiation of intestinal epithelium and continued elongation with growth.

1.2 *The Intestinal Wall*

As the intestinal structures develop from the primitive gut tube, the four layers of the intestinal wall form (Figure 1). From the lumen outward these are the mucosa, submucosa, muscularis externa, and the serosa. The mucosa spans the epithelium which faces inwards towards the lumen, lamina propria which separates the thin muscle of the muscularis mucosae from the epithelia. The submucosal layer supports the muscularis with a collagen based extracellular matrix and houses some ganglia found in the submucosal plexus. The muscularis externa is composed mostly of muscle that is controlled by the ganglionic neurons surrounding it; this allows it to contract and expand in a circular/longitudinal manner to pass waste through the intestinal tract. It contains the myenteric plexus which is one of the innervated layers. The final layer is the serosa which is a bilayered membrane which binds the muscularis externa together and serves as a base of support of the GIT (Heath 2010).

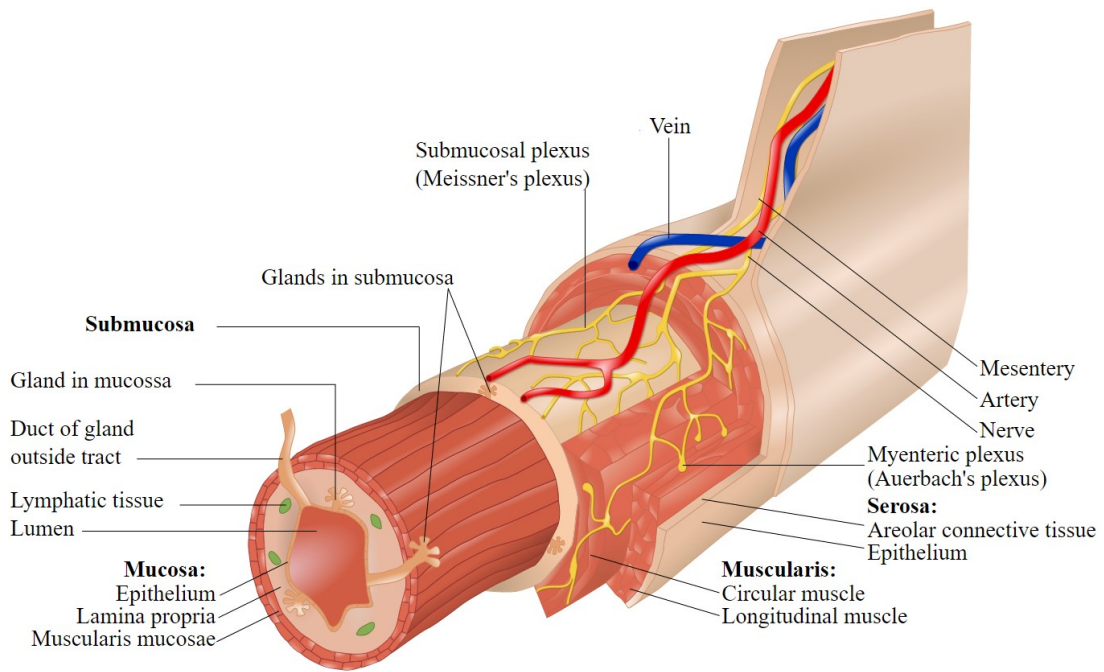


Figure 1. Representation of the layers of the intestinal wall. This figure describes the four main layers, the mucosa, submucosa, muscularis and the serosa, as well as their components. Adapted from OpenStax, Anatomy & Physiology. OpenStax CNX. Feb 26, 2016.

Download for free at <http://cnx.org/contents/14fb4ad7-39a1-4eee-ab6e-3ef2482e3e22@6.27>.

1.3 *The Intestinal Epithelium*

The intestinal lumen is lined by an epithelium that is the site of contact with the partially digested food products (chyme) entering from the stomach. This environment is particularly harsh as there are mechanical complications from the chyme passage, chemical balances to facilitate digestion/absorption, and immunological responses to microbes throughout the lumen. The epithelium is therefore strictly regulated in terms of cell content and renewal as determined by the intestinal segments' role. The small intestine takes on the majority of the digestion and nutrient absorption roles, with the duodenum participating most in digestion of chyme, while the jejunum and ileum absorb nutrients from the products of digestion (Solomon, Berg et al. 2002). The large intestine does not primarily participate in nutrient uptake, instead absorbing most of the remaining water and salts from the waste before it is excreted (Sandle 1998). These differences result in specialized cell types found in varying proportions depending on the organ.

Throughout the intestine there are four major cell types: enterocytes (absorptive), enteroendocrine, goblet (mucosecretory), and Paneth (Sancho, Battle et al. 2003). Enterocytes are found only in the small intestine as they are the absorptive cells of the intestine, making up an estimated 80% of the epithelium of the small intestine. Additional roles are maintaining the structure of the epithelium through tight-junctions as well as antigen uptake and processing (Snoeck, Goddeeris et al. 2005). Enteroendocrine cells make up about 1% of the GIT, and are chemosensors responsible for communicating with the ENS through secretion of gastrointestinal hormones. Secretion is activated upon detection of luminal contents and can facilitate physiological changes, as well as homeostatic ones through this communication (Gribble and Reimann (2016), Latorre, Sternini et al. (2016)). Goblet cells are mucosecretory cells found in greater numbers more distally through the intestinal tract, contributing about 4% of the duodenal epithelium, and 16% of the distal colon (Chang and Leblond 1971). The mucous secreted by these cells serves to protect the epithelium from the mechanical scraping it undergoes as waste is passed, which is why they are found in greater numbers in the colon, where there is less water present in the waste. Paneth cells are found in the base of the intestinal villus structure, the Crypts of Lieberkuhn in the small intestine. Their role is primarily regulation of the intestinal microflora, producing secretory granules packed with antimicrobial peptides that serve to protect the epithelium from harmful bacteria, while modulating positive microflora that aid in digestion

(Ayabe, Satchell et al. 2000). In the small intestine each of these four lineages are found; enterocytes (absorptive), enteroendocrine, goblet (mucosecretive), and Paneth cells, making the small intestine the major site of absorption and digestion within the intestine (Figure 2A) (Potten 1998). The colon is comprised predominantly of mucosecreting cells (goblet) and enteroendocrine cells which together are known as colonocytes (Figure 2B) (Sancho, Batlle et al. 2003)

There remain a few distinct cell types that make up the remainder of the intestinal epithelium. Microfold cells are enterocyte-like, and found only in the small intestine. They are involved in the uptake and transportation of antigens and peptides from the lumen, but specifically communicate with macrophages to initiate an immune response (Gebert, Rothkotter et al. 1996). Cup cells are the least studied cell in the small intestine, present predominantly in the ileum; their role in the epithelium is currently unclear (Madara 1982). The last cell type of the intestinal epithelium is the tuft cell. Tuft cells are typically present in low levels but are suspected to contribute to the intestinal immune response, as they have been shown to accumulate in greater numbers during infections (Hofer and Drenckhahn 1996, Reid, Meyrick et al. 2005).

As the intestinal epithelium is constantly being shed these cells need to be continually replenished. The Crypts of Lieberkuhn house the intestinal stem cells that facilitate this turnover (van der Flier and Clevers 2009).

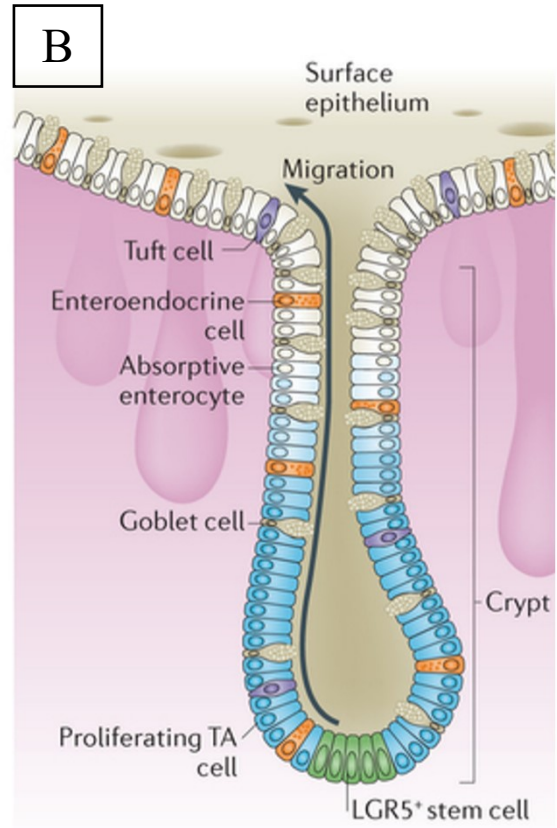
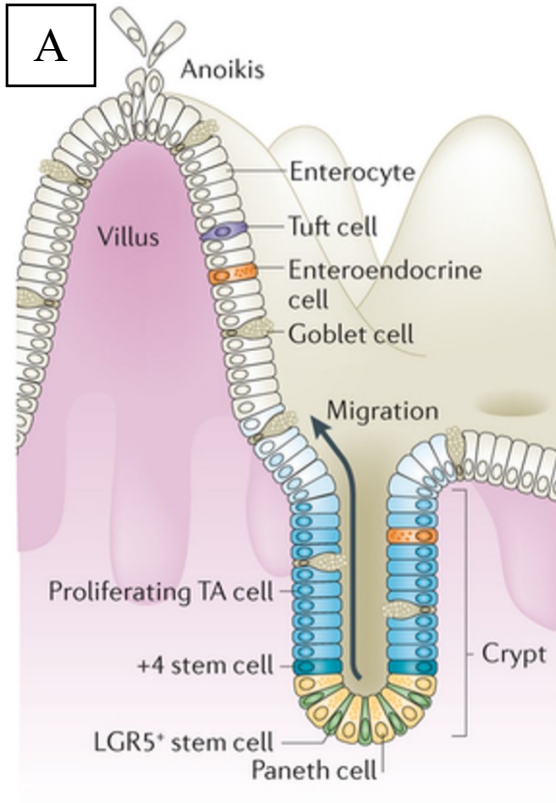


Figure 2. The intestinal stem cell niche of the Crypts of Lieberkuhn in the small and large intestines. A) The small intestine stem cell niche is composed of differentiated Paneth cells and stem cells at the base, which become transit amplifying cells that either migrate upwards and differentiate into the epithelial cell types, or downwards to replace Paneth cells. B) The large intestine stem cell niche does not contain Paneth cells, as that cell type does not differentiate out of the transit amplifying cells (TAs). The lack of a villus is also apparent with cells migrating out of the crypt into an unraised epithelium.

Adapted from Barker, 2014 (Nature), Permission reference [4142000667505](#)

1.4 Intestinal Stem Cell Niche

In the mature intestine, stem cells are contained within the Crypts of Lieberkuhn. This is a compartmentalized structure, made up primarily of intestinal stem cells (ISCs), Paneth cells, and TA cells as depicted in Figure 2. In the small intestine, there are six crypts per villi which replenish the differentiated epithelium as cells migrate upwards out of the crypt. The exceptions to these cells are those that differentiate into Paneth cells, which migrate back into the base of the crypt in the small intestine (Figure 2A) (Shaker and Rubin 2010, Barker 2014). In the large intestine there are no Paneth cells in the crypt; it remains composed predominantly of stem cells and their TA cells leading into differentiated epithelium (Figure 2B) (Barker 2014). The current model for ISCs indicates two populations of stem cells in the crypt: actively cycling cells that generate the TAs and quiescent reserve stem cells that replace the cycling cells (Tian, Biehs et al. 2011). The actively dividing population is marked by *Leucine-rich repeat-containing G-protein coupled receptor 5 (Lgr5)*, as shown by lineage tracing experiments, and found below the +4 cell position of the crypt known as Crypt Basal Cells (Figure 2) (CBCs) (Barker, van Es et al. 2007). LGR5 is a canonical WNT signalling pathway ligand, interacting with R-spondin upon ligand binding to activate Beta Catenin and downstream targets (de Lau, Peng et al. 2014). The second stem cell type is a reserve population maintained in a quiescent state at the +4 position of the crypt (q-ISCs) as depicted in Figure 2A (Tian, Biehs et al. 2011). These cells are necessary to maintain proper crypt structure, and can even restore the cycling stem cell population in the event of damage/loss of the *Lgr5* population (Richmond, Shah et al. 2016). Originally thought to be marked by *B lymphoma Mo-MLV insertion region 1 homolog (Bmi1)*, a Polycomb Repressive Complex 1 (PRC1) protein, *Bmi1* is no longer considered a stem cell marker, being expressed in both CBCs and q-ISCs (Sangiorgi and Capecchi 2008, Zhang and Huang 2013, Barker 2014). Multiple potential markers have been suggested for q-ISCs, such as *mTert*, *Sox9* and *Lrig1*; however, no single consensus marker has been identified (Formeister, Sionas et al. 2009, Montgomery, Carlone et al. 2011, Powell, Wang et al. 2012) This population has been shown to restrict WNT signalling and arrest in G1 of mitosis, while activating the BMP signalling pathway. Inhibition of BMP-4 in the intestine has also been shown to result in the generation of ectopic crypts likely due to the loss of regulation of q-ISCs (Richmond, Shah et al. 2016).

1.5 *Bmi1* and the Polycomb Repressive Complex

When this project was initiated *Bmi1* was considered a reliable intestinal stem cell marker of q-ISCs (Yan, Chia et al. 2012), and had been shown to co-localize with DLX2 in the intestinal crypt as seen in Figure 14A&B (Fonseca and Eisenstat, unpublished). It was therefore selected as a potential DLX2 target within the developing intestine based on the data of the time and its role as a Polycomb group gene (PcG). PcGs are typically divided based on their interactions with the two Polycomb Repressive Complexes (PRC1, PRC2) which work together to silence genes through chromatin remodelling. The specific mechanisms through which these complexes act to remodel chromatin are not entirely clear, with questions about complex recruitment to genes and repression initiation being poorly defined (Mahmoudi and Verrijzer 2001). Each complex consists of a core set of proteins, with a multitude of secondary binding partners to modify histones. It is thought that some of these secondary binding partners contribute to target selection. PRC2 has three core components; EZH2, SUZ12 and EED. EZH2 is a histone methyltransferase, and is responsible for trimethylation of lysine 27 on histone 3 (H3K27me3) of the nucleosome (Kuzmichev, Nishioka et al. 2002, Margueron and Reinberg 2011). This methylation event has been well characterized as inducing gene silencing as well as being a recruiter of Cbx (chromobox homologue) chromodomains (Cao, Wang et al. 2002). CBX proteins are members of the PRC1, and are believed to position the complex at target genes based on their interactions with H3K27me3 sites (Gao, Zhang et al. 2012). Other core proteins of the complex include BMI1, RING1A/B and RYBP (RING1 binding protein) (Gray, Cho et al. 2016). Together the PRC1 complex contributes to chromatin folding through the mono-ubiquitination of histone 2A Lysine 119 (H2AK119ub1), mediated by RYBP (Nakagawa, Kajitani et al. 2008). These modifications contribute to the condensation of DNA around the nucleosome due to increased covalent bond strengths, silencing genes by restricting the access of transcriptional machinery to the promoter regions. PRC1 can reach targets in other ways, such as through KDM2b (Lysine Demethylase 2B) mediated recruitment to unmethylated CpG islands, or through BMI1 recruitment by the transcriptional machinery (Farcas, Blackledge et al. 2012, Yu, Mazor et al. 2012, Gray, Cho et al. 2016). Additional ways for PRC1 to differentiate targets are being investigated, but a major contributor to the variety seen is due to the variability in PRC1 components. Many of the core proteins are interchangeable with their family members, for

example CBX-2, -6, -4, -7, and -8 can each fill the CBX protein role in the complex (Gao, Zhang et al. 2012).

1.6 *Intrinsic innervation of the GIT by the neural crest*

The Enteric Nervous System (ENS) is composed of a network of neurons and glial cells organised across two layers of GIT wall. The Myenteric Plexus (Auerbach plexus) and the submucosal plexus house the ENS cells (Fig. 1), which are derived from the neural crest cells (NCC). The neural crest forms from the ectoderm as the neural plate folds to form the neural tube (Uesaka, Young et al. 2016, Nagy and Goldstein 2017). Vagal and sacral NCCs migrate into the foregut by E9 in mice, corresponding to week 4 in humans (Montgomery, Mulberg et al. 1999). Upon entry into the foregut vagal NCC cells are renamed Enteric Neural Crest-Derived Cells (ENCC). This migration is driven by retinoic acid produced from the mesoderm which in turn upregulates the expression of the *Ret proto-oncogene* receptor tyrosine kinase (Fu, Sato et al. 2010, Simkin, Zhang et al. 2013). In turn, RET and its co-receptor Glial Derived Neurotrophic Factor $\alpha 1$ (GDNF $\alpha 1$) are activated by the ligand GDNF, creating a phosphorylation chain activating several cell signalling pathways such as MAPK, JNK and PI3K that drive innervation through the GIT through their downstream targets (Figure 3, Figure 4) (Jing, Wen et al. 1996, Takahashi 2001). Sacral NCCs take on a supporting role in some species, but not others. In mice, they only enter the hindgut after it has been colonized by vagal ENCCs, and contribute almost solely to distal neuronal makeup in the hindgut (~17%) (Burns and Douarin 1998). The role of sacral NCCs in human innervation is still unknown.

The PI3K pathway has a large role in ENS development, contributing extensively to ENCC migration and survival. Expression of its downstream effector Rac1 induces actin lamellipodia formation, which is what allows the ENCCs to migrate through the GIT. ENCC survival is influenced by the PI3K/AKT pathway via GDNF, meaning that the proliferative ability of the ENCC migratory wave is limited by GDNF availability (Du, Wang et al. 2009, Du and Liu 2015). Inhibition of PI3K arrests cell migration and can cause aganglionosis. Its inhibitor PTEN is expressed in cells proximal to the leading edge of the migratory wave, and its expression contributes to the decision of an ENCC to halt migration and to begin differentiation (Fu, Sato et al. 2010). ENCC differentiation produces two enteric cell families, enteric neurons and enteric

glia. The neurons maintain *Ret* expression and differentiate into four sub-types, the glia cells lose *Ret* expression and differentiate into the supporting cells for the neurons (Figure 3).

The last major contributing pathway is the Endothelin Receptor B (EDNRB) pathway. This pathway is responsible for maintaining the ENCC proliferative state by inhibiting differentiation (Barlow, de Graaff et al. 2003). Its ligand, ET-3 is expressed by the gut mesenchyme and acts synergistically with GDNF to aid in proliferation via this inhibition (Nagy and Goldstein 2006). Interestingly, it has been shown to inhibit the chemoattractive effect of GDNF on ENCCs, which suggests some role in the decision to stop migrating through the tube (Wu, Chen et al. 1999, Nagy and Goldstein 2006, Mwizerwa, Das et al. 2011). The EDNRB pathway has received less attention than the RET signalling pathway when investigating innervation due to the significance of RET in Hirschsprung's Disease, (HD) and so there is less known about the specific mechanisms that it works through. The EDNRB pathway accounts for an estimated 5% of HD cases, while RET is involved in nearly 75% of cases (Tam and Garcia-Barcelo 2009).

Innervation continues moving from the proximal foregut towards the distal colon from E9 to E12.5, innervating the GI tract as it grows and develops. In humans, the intestinal tract is innervated by ENCCs by week 7 of gestation. Innervation is not complete until the ENCCs have differentiated into their final cell types, which is determined by the expression of various transcription factors downstream of the signalling pathways (Furness 2000, Anderson, Stewart et al. 2006).

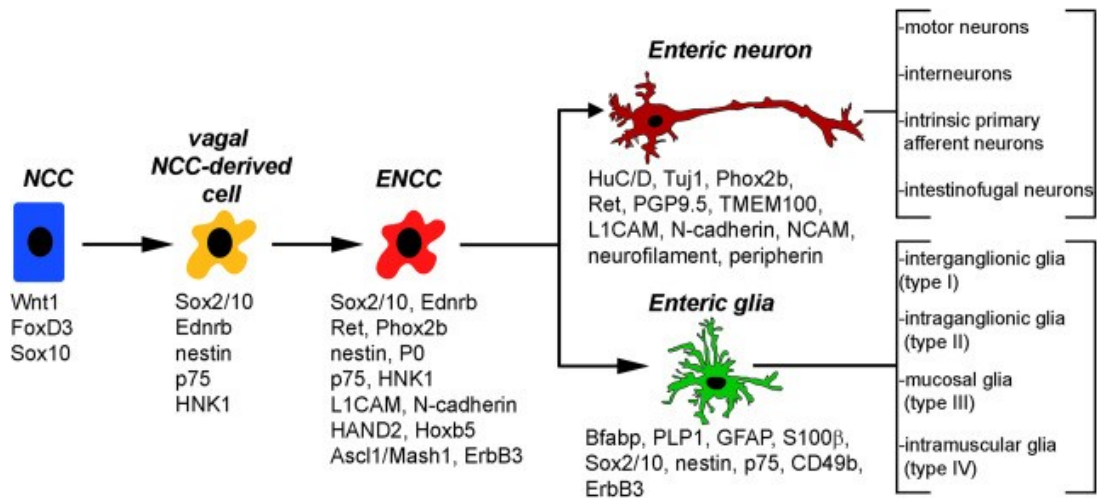


Figure 3. Differentiation of Neural Crest Cells into enteric neuronal and glial subtypes.

This figure shows the progression of neural crest derived cells and the changes to the genes they express as they migrate and differentiate away from the NCC towards their finalized ENS role.

Adapted from Nagy & Goldstein, 2017. Permission reference [4142000435506](#)

1.7 The *Ret* proto-oncogene

Proto-oncogenes are those genes that undergo mutations resulting in oncogenic effects, most often because of gain of function alterations. Named *rearranged during transcription (ret)*, the *Ret* gene has 21 exons and is located on chromosome 10. It encodes a tyrosine receptor kinase with three domains: the extracellular N terminal interacts with ligands, a transmembrane domain, and a cytoplasmic tyrosine domain (Takahashi, Ritz et al. 1985). The extracellular region contains cadherin-like domains that facilitate binding to the ligand using Ca^{2+} ions (Anders, Kjar et al. 2001). The ligand for RET are glial derived neurotrophic factors (GDNFs). While GDNF is the most well studied ligand, some other members of the GDNF ligand family have been shown to bind and activate RET (Jing, Wen et al. 1996). Binding is facilitated by GDNF receptor α ($\text{GFR}\alpha$), a membrane anchored protein that forms a complex with GDNF, which then recruits two RET molecules that then dimerize and initiate auto-phosphorylation of the cytoplasmic domain at tyrosine 1062 (pY1062), as depicted in Figure 4. This results in signal transduction throughout the rest of the pathway (Takahashi 2001, Kawamoto, Takeda et al. 2004). There are a variety of downstream pathways, such as those mentioned in the previous section on innervation, as well as the RAS/RAF targets of the MAPK pathway. Many downstream effectors of RET activation are genes involved in promoting cell survival and proliferation.

It is no surprise that over-expression of RET has oncogenic effects. While *de novo* cases are relatively low, inherited RET mutations that cause a gain of function are autosomal dominant when inherited, and give rise to all sub-types of multiple endocrine neoplasia type 2 (MEN2). MEN2 has three sub-types: MEN2A, MEN2B and familial medullary carcinoma of the thyroid (FMTC). MEN2A typically results from RET mutations inducing dimerization independently of ligand binding, resulting in constitutively active signal transduction (Marquard and Eng 1993, Mulligan, Kwok et al. 1993). It is the most common MEN2 subtype, accounting for upwards of 70% of cases, and typically presents with MTC and/or hyperthyroidism (Eng, Clayton et al. 1996). Individuals with MEN2A can also develop pheochromocytoma either concurrently or more commonly after MTC development (Inabnet, Caragliano et al. 2000). Mutations resulting in phosphorylation of the tyrosine kinase domain of RET without dimerization cause MEN2B, as can mutations resulting in constitutively active RET without a proper ligand binding (Cranston, Carniti et al. 2006, Gujral, Singh et al. 2006). MEN2B is the least common form of MEN2, with

cancers developing early in lifehood. It is commonly diagnosed in childhood as affected individuals develop mucosal neuromas and submucosal nodules on craniofacial features (Soroa-Ruiz, Lara-Sanchez et al. 2014). MTC occurs when the RET effectors MAPK and PI3K pathways are constitutively active (Eng, Clayton et al. 1996).

As previously discussed, *Ret*'s normal role in development is to drive NCC migration and survival to innervate the GI tract. When mutations cause a reduction of *Ret* expression this innervation is disrupted and can lead to the developmental disorder Hirschsprung's Disorder.

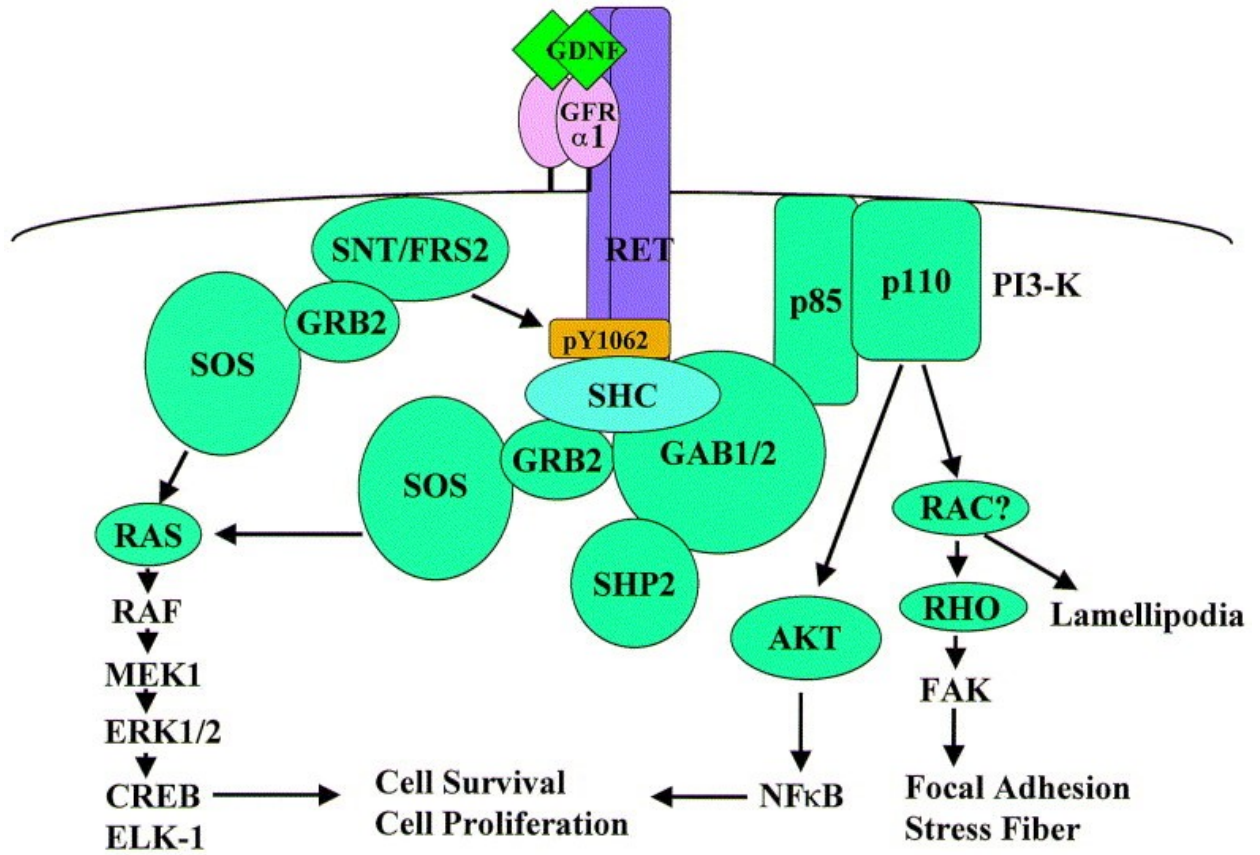


Figure 4. Cell signalling cascade involved with the GDNF RET signalling pathway. The intracellular effectors of the GDNF RET pathway. Figure shows dimerized RET activated by phosphorylation at tyrosine 1062 (pY1062) and the various downstream signalling pathways effected.

Adapted from (Takahashi 2001). Permission reference [4142000574200](#)

1.8 Hirschsprung Disorder

Hirschsprung Disorder (HD) is an intestinal developmental disorder of the Enteric Nervous System, typically restricted to the distal colon. Typically caused by a failure of ENCCs to innervate the distal colon, HD is characterized by an aganglionic segment of intestine. A truly aganglionic region has no ganglion cells in either the myenteric or submucosal plexi and can also be missing parasympathetic nerve fibres (Amiel, Sproat-Emison et al. 2008, Schriemer, Sribudiani et al. 2016). Typically HD is detected during the neonatal period as a result of delayed or non-passage of the meconium, and treated with resection of the aganglionic segment (Sergi, Caluseriu et al. 2017). In severe cases a colostomy is necessary if the aganglionic region is too large to be resected. This has created the classifications of short and long segment HD (Alnajjar, Murro et al. 2016). Short segment HD is classified as having the aganglionic section of bowel restricted to the rectosigmoid colon. Long segment HD aganglionosis extends into the sigmoid colon. Together, long and short segment HD make up 95% of cases, with the remaining 5% of patients presenting with an entirely aganglionic large intestine (Badner, Sieber et al. 1990). Current treatment options are limited to select options such as segmental resectioning of GIT tissue or colostomy. Surgery is invasive and typically performed early in the neonatal period, and so there is an interest in discovering alternative treatment options, such as the novel use of indwelling transanal tubes (ITTs) to clear the bowel prior to surgeries, or the use of ENS stem cells and implantation techniques to repopulate the ganglion of the affected area (Metzger, Caldwell et al. 2009, Mochizuki, Shinkai et al. 2017).

Most HD cases are sporadic, with only 5-20% being familial while it presents as an isolated case 70% of the time. Its incidence is estimated at 1 in 5000 live births worldwide, with males being affected at a rate of 4:1 when compared to female prevalence in short segment HD (Amiel, Sproat-Emison et al. 2008, Moore 2016, Bradnock, Knight et al. 2017). While there are a variety of causes for HD, the most common factor is loss of function of the *Ret proto-oncogene* (Hofstra, Wu et al. 2000, Gabriel, Salomon et al. 2002, Uesaka, Nagashimada et al. 2008). Please refer to the innervation of the intestine section for the role that *Ret* plays in intestinal innervation. As of 2005, there had been greater than 116 different HD causing mutations identified in *RET* from patient samples. Figure 5 shows that a sampling of these mutations does not reveal any specific mutation hotspot on the *RET* gene. Attempts to use this information to predict the correlation of

RET mutations to the severity of HD have therefore been difficult (Hofstra, Wu et al. 2000, Gabriel, Salomon et al. 2002, Kashuk, Stone et al. 2005). In part this difficulty is due to the fact that most cases of HD are the result of non-complementary second site mutations. Recently a cause of the increased propensity for males to present with short segment HD was discovered. *Ret* is known to be activated by SOX10 co-activation of the transcription factors PAX3 and NKX2-1 (Leon, Ngan et al. 2009). Sox10 is a member of the Sex determining factor Y (SRY) - box genes, which share a conserved DNA binding domain with the male sex determining factor SRY (Bowles, Schepers et al. 2000). SRY has been discovered to compete with Sox10 to form complexes with PAX3 and NKX2-1, resulting in repression of their regulation of *Ret*, which exacerbates HD aganglionosis in males (Li, Kido et al. 2015). Of note, both PAX3 and NKX2-1 are homeodomain containing transcription factors, as is DLX2, our regulator of interest (Sheng, Harris et al. 1997, Stanfel, Moses et al. 2005).

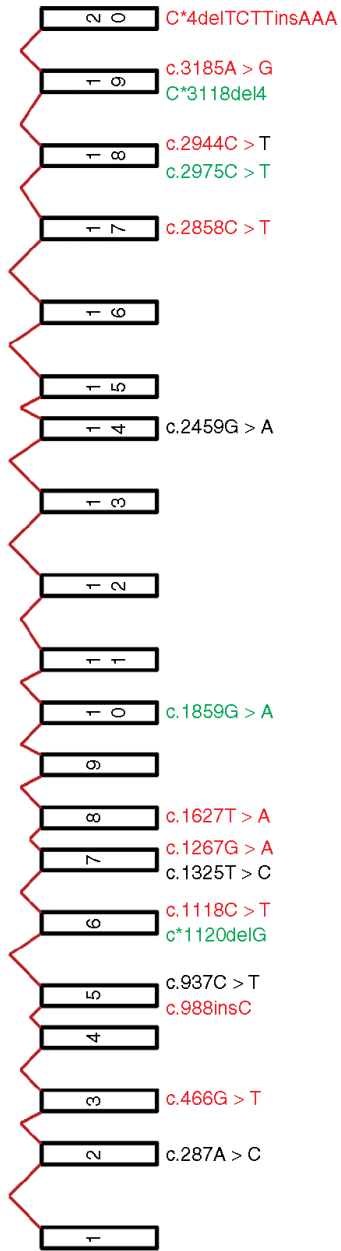


Figure 5. Mutations of *RET* and their effects on patient presentation of Hirschprung's Disease. Multiple reported and confirmed pathological mutations affecting the *RET* locus have been presented with their general locations in the exons of the gene. Mutations written in red have been associated with short segment HD, those in green with long segment HD, and those in black were reported as pathogenic causing aganglionosis but without reports of segment analysis. Adapted from (Sergi, Caluseriu et al. 2017).

1.9 Homeobox genes

The homeobox genes are members of a gene family of transcription factors that contain a conserved 60 amino acid DNA binding domain known as the homeodomain. This domain recognizes a generalized tetranucleotide DNA binding motif of TAAT/ATTA, and binds it via two of the four helices that make up the homeodomain (Kraus and Lufkin 2006). This family was first identified in *D. melanogaster* and are famously known for the *Homeobox (Hox)* genes, which order embryonic development along the anterior-posterior axis (Carrasco, McGinnis et al. 1984). The sub-group of homeobox genes we are interested in are the *distal-less homeobox (DLX)* genes. In mouse and human there are six *Dlx* genes; these are located in bigenic clusters pairing two genes: *Dlx1* & *Dlx2*, *Dlx3* & *Dlx4*, and *Dlx5* & *Dlx6*. Additionally, each of these pairs are themselves linked to a specific *Hox* gene locus, *Hoxd* to *Dlx1/2*, *Hoxb* to *Dlx3/4*, and *Hoxa* to *Dlx5/6* (Stock, Ellies et al. 1996). Our interest lies with *Dlx1* and *Dlx2* and their role in the developing intestine as well as other developing organ systems.

Dlx1 and *Dlx2* are located closest together, their bigenic cluster sharing an enhancer region and each containing 3 exons, 2 introns on the p arm of chromosome 2 (McGuinness, Porteus et al. 1996). These genes appear to be somewhat functionally redundant, while still maintaining some separation of function through overlapping but sequential patterning (Qiu, Bulfone et al. 1997). This partial redundancy is seen in single knockout (KO) mice that have been generated for *Dlx1* and *Dlx2*, as there are only minor visible phenotype despite the KO mice dying at birth (postnatal day 0, P0), most likely due to the functional redundancy of the genes (Eisenstat, Liu et al. 1999). Visible phenotypes are more severe when these two genes and their bigenic enhancer are knocked out in tandem, generating the *Dlx1/2* DKO mouse, which presents with a cleft palate, distended GI tract (Fig, 6), reduced retinal ganglia cell layer (de Melo, Du et al. 2005) and a loss of the GABAergic interneuron migration towards the neocortex. The distended GI tract is of interest to this project as it is a similar phenotype to a megacolon, in that there is possibly a blockage occurring that is causing the GIT to expand proximal to the blockage site. This could be occurring in a manner similar to HD, where an aganglionic region causes waste buildup and leads to the eventual megacolon phenotype. There is also unpublished data from the Eisenstat lab that indicates a role for *Dlx1/2* in the developing pancreas, which shares the same origin as the intestine, arising from the endoderm. Additional unpublished data has characterized *Dlx2*

expression in the developing intestine, finding its expression to be restricted to the Auerbach's ganglia from embryonic day 13 (E13) until embryonic day 18 (E18) when DLX2 appears in the intestinal epithelia (Fonseca & Eisenstat unpublished data).



Figure 6. DLX1/2 Double knockout mouse P0 pup. The distended GI tract phenotype of the P0 double knockout mouse pup is highlighted in this figure. This is the most obvious external phenotype of the embryo, which does not survive past P0. Other phenotypes include a cleft palate, thinning of the retinal ganglion layer and disruptions to GABAergic interneuron migration.

Adapted from Dr. David Eisenstat (unpublished data)

Chapter 2: Hypothesis and Research Aims

2.1 Hypotheses

Immunostaining assays on developing intestinal tract revealed DLX2 to be expressed in the Auerbach's ganglia, as well as the intestinal epithelium in late prenatal development. Subsequent chromatin immunoprecipitation assays (ChIP) revealed the *Ret* and *Bmi1* regulatory regions to be occupied by DLX2 during development in these embryonic tissues.

We therefore hypothesize (1) that DLX2 directly binds the *Ret* and *Bmi1* regulatory regions to transcriptionally activate *Ret* expression at embryonic day 13, and repress *Bmi1* expression at E18.5. We also hypothesize (2) that in the absence of DLX2 there is abnormal ENS development.

2.2 Aim 1: Determine the co-localization of DLX2 with *Ret* and *Bmi1* in cell types of the intestinal tract

Dual immunofluorescence assays were performed on both mouse and human tissue to determine if there is co-expression of DLX2 with either of these proteins in the developing intestinal tract. Antibodies specific to DLX2, RET and BMI1 were used in conjunction with other cell type markers to determine what subset of intestinal cells express these proteins.

2.3 Aim 2: Determine the specificity of the interactions between DLX2 and the target regulatory regions during development.

Chromatin immunoprecipitation assays using a specific polyclonal antibody against DLX2 were performed on the embryonic intestines at varying time-points to determine occupancy of the *Ret* and *Bmi1* regulatory regions. Following this electrophoretic mobility shift assays (EMSA) were performed to determine the capacity of DLX2 to bind directly to radiolabelled regulatory region DNA fragments of the target genes identified by ChIP *in vitro*.

2.4 Aim 3: Determine the regulatory role that DLX2 has on the transcription of the gene targets.

Luciferase gene reporter assays were performed to determine the *in vitro* functional effect of DLX2 on the specific regulatory region fragments by co-transfection of a *Dlx2* expression plasmid with ChIP-isolated, EMSA verified target fragment containing reporter vectors into

HEK293 cells. The biological role of DLX2 over the expression of these two genes was determined by quantitative real time PCR. RNA was isolated from embryonic DLX1/2 DKO and WT mouse intestines, and transcript levels of *Ret* and *Bmi1* measured to determine the effect of loss of DLX1/DLX2 on gene expression.

Chapter 3: Material and Methods

3.1 *Animal and Tissues Collected*

Both human and mouse (*mus musculus*) tissues were used in the study presented. Tissue from mice was taken at two embryonic ages to initially evaluate a range of developmental stages. Embryonic ages 13.5 & 18.5 (E13.5/E18.5) were the selected ages, using gastrointestinal tissue for the studies, as well as ganglionic eminences from the embryonic forebrain as control tissue for the chromatin immunoprecipitation (ChIP) experiments. Tissue used in the ChIP experiments was taken from timed pregnant CD-1 Swiss mice ordered from the Charles River Laboratory, while the *Dlx1/Dlx2* double knock out (DKO) transgenic mice were utilized to obtain tissue for investigations into transcriptional regulation. Pregnancy was determined by the presentation of a vaginal plug in the dam mouse, marking day 0.5 of pregnancy. To obtain embryonic tissue dams were sacrificed at the appropriate time points through cervical dislocation followed by embryo removal. Embryos were euthanized through decapitation upon removal and had the appropriate tissues extracted through dissection. When using DKO mice, genotyping was performed to determine which littermates were of a WT and which were *Dlx1/Dlx2* DKO genotypes. Heterozygote mice were not used in these studies.

Human Tissue was provided by Dr. C. Sergi (U. Alberta) and Dr. Grynspan (U. Manitoba), freshly removed from patients. It was then further cut into smaller sizes for fixation and sectioning.

All experiments using CD1 or DLX1/2 DKO mice were approved by the University of Alberta animal care user committee. All human tissues were obtained with approval by the Human Research Ethics Boards at the U. Manitoba or U. Alberta.

3.2 *Tissue Preparation, Fixation & Sectioning*

Mouse intestinal tissues dissected for sectioning were cleaned and rinsed with 1X Phosphate Buffer Saline (PBS) to remove faecal and other undesirable matter from the GI tract, followed by fixation with 4% paraformaldehyde (PFA) overnight at 4° Celsius (C) with gentle rotation. Tissues were then run through a sucrose gradient of 15% to 20% and lastly 30% at 4°C prior to embedding. Tissue remained at each step of the gradient until it was saturated and deposited at the bottom of the vial, remaining in 30% sucrose until being embedded for sectioning. Prior to

embedding, tissues were incubated in a 50:50 mixture of 30% sucrose and Optimal Cutting Temperature Compound (OCT) purchased from VWR for 30 minutes at room temperature. Tissues were then frozen into blocks using 100% OCT and stored at -80°C until sectioned.

Sectioning was performed using a Cryostat Leica CM 3000 cutting at 10µm and placing tissue on Superfrost Plus slides (Fischer Scientific). Sectioned slides were stored at -80°C in sealed containers until use in immunostaining.

Human tissue was fixed overnight at 4° Celsius, and then treated in the same manner as mouse tissues for sectioning.

3.3 Chromatin Immunoprecipitation

Chromatin immunoprecipitation assays (ChIP) were carried out on mouse embryo whole intestine and hindbrain at two age points (E13.5 and E18.5), from timed pregnant CD-1 mice. Hindbrain was taken as a negative control as there is no DLX2 expression in the developing hindbrain, while the GIT was considered the experimental tissue. Upon dissection, all tissues were rinsed with cold 1x PBS, the GIT lumen was given an additional wash by flushing 1xPBS through the tract to clear any non-intestinal matter. Cells were then dissociated into a single cell suspension by repeated passaging through a 24 Gauge needle prior to fixation, and prepared for the ChIP assay as per Zhou *et al* (2004).

1% paraformaldehyde (PFA) plus Protease Inhibitor Cocktail (PIC) was used to induce crosslinking in the cells at room temperature for 30 minutes for both cell types. Cells were washed twice with 1x PBS and centrifuged at 2500 rpm for collection (this centrifugation speed is used unless otherwise stated). Cells were then lysed using 400µl of a 1% SDS, 10mM Tris-HCL (pH 8.1), and 10mM EDTA buffer plus PIC. The method used to shear the DNA was sonication using a 60 Sonic Dismembrator at 40% output strength. Samples were sonicated on ice for 15s intervals followed by 30s rests to avoid over heating the DNA. DNA band size of 300 – 500bp fragments was confirmed by running 5µl of sheared DNA on a 1% agarose gel (data not shown).

Pierce UltraLink Protein A/G beads were used to remove immunoglobulin Gs (IGGs) from the tissue prior to incubation with concentrated DLX2 antibody (DDE, proprietary). 60µl of beads per sample tube were washed with 1ml of dilution buffer of 0.01% SDS, 1.1% Triton X-100, 1.2mM EDTA, 16.7mM Tris-HCl pH8.1, 167mM NaCl and PIC, and prepared to a 50% concentration of beads in buffer. 60µl of these beads were added to each sample tube and rotated at 4°C for 1 hour. Samples were then centrifuged and the supernatant transferred to new tubes. Beads are then discarded.

To this supernatant 500µg/ml of BSA and tRNA are added, designated tubes also receive 2µl of concentrated DLX2 antibody, whereas negative controls receive no antibody. These tubes are incubated at 4°C overnight with rotation. At the same time A/G beads are prepared in the same manner as above, with the addition of 500µg/ml of BSA and tRNA to the buffer. These beads are incubated at 4°C overnight with rotation. On the following day 60µl of beads are added to each tube and left for 24 hours with rotation at 4°C. At the end of this incubation DNA-protein complexes containing DLX2 are bound by the antibody and attached to the beads, and unbound complexes are found in the supernatant. Beads are pelleted by centrifugation and separated from the supernatant which is saved as Total Input and stored at -20°C.

The beads undergo a series of washes with rotation at 4°C prior to elution of the antibody bound complexes. Low salt buffer for 5 minutes (0.1% SDS, 1% Triton X-100, 2mM EDTA, 20mM Tris-HCl pH8.1 and 150mM NaCl) is the first wash, followed by High salt buffer (0.1% SDS, 1% Triton X-100, 2mM EDTA, 20mM Tris-HCl pH8.1 and 500mM NaCl) for 30 minutes, then a LiCl buffer (0.25M LiCl 1% deoxycholate, 1mM EDTA, 10mM Tris-HCl and 1% NP-40) wash for 30 min and finally two 5 minute washes with TE buffer (pH 8.0).

After removing the buffer from the last wash complexes are eluted from the beads by administration of 250µl of Elution buffer (1% SDS, 0.1M NaHCO₃) pre-warmed to 65°C and left for 15 minutes with agitation. Samples are spun down and the supernatants collected into fresh tubes. This step is repeated once more and the respective supernatants combined into appropriate tubes. The supernatants now contain DLX2 antibody bound DNA-protein complexes, and should have ~ 500µl volumes. 1µl of RNaseA and 25µl of 5M NaCl are added and the samples incubated at 65°C overnight. The following day 10µl of 0.5M EDTA, 20µl of 1M Tris-HCl (pH 6.5) and 2µl of Proteinase K are added to the samples and incubated for 2 hours at 65°C. This

reverses the crosslinking and degrades the protein structures, leaving only candidate DLX2 targets. The samples are then purified using a QiaQuick PCR purification kit (Qiagen) and can undergo PCR amplification of suspected DLX2 target regions using primer sets described in Table 1.

3.4 Molecular Cloning

Regulatory regions identified through the *in vivo* ChIP assay were then taken to be cloned into the pGL3- Basic Vector (Promega) reporter plasmid for use in multiple later studies. Primers used in the ChIP assay were modified with the addition of appropriate restriction sites (Table 2.) to the 5' and 3' primer sets. The addition of these sites allows for the creation of overlapping “sticky” ends for direction specific ligation into the vector’s multiple cloning site. Regions were PCR amplified with Phusion Polymerase (NEB) from CD-1 genomic DNA, and purified using a QIAquick PCR Purification Kit (Qiagen). 500ng of each DNA region was digested using 1 unit of appropriate restriction enzymes, 4µl of NEB Buffer, 4µl of 10X BSA to a total volume of 20µl for two hours at 37°C. Empty pGL3 was digested simultaneously with the matching enzymes to the regions to create compatible overhanging DNA ends. Digested plasmid and regions were isolated by gel electrophoresis on 1% agarose gels and cleaned with QIAquick Gel Extraction Kits (Qiagen). Insertion of digested region DNA into matching pGL3 vectors was performed using T4 DNA ligase at a vector molar ratio of 3:1 insert to vector for optimal ligation.

This ligation mix was then used to transform competent DH5α *E. coli* cells by introducing 3µl of ligated plasmid to 30µl of bacteria and incubating for 30 minutes on ice. Following this incubation, the bacteria was heat shocked at 42°C for 1 minute and returned to ice for 5 minutes, followed by a recovery period of 2 hours at 37°C in Lysogeny Broth (LB) media with rotation. Cells were then plated by spreading 250µl of media onto LB agar plates containing 50mg/ml carbenicillin to select for resistant colonies. Plates were incubated at 37°C overnight.

The next day single colony units were picked for inoculation into LB broth + carbenicillin, and grown at 37°C overnight with rotation. Plasmids were isolated from cells the next day using a QIAprep Spin Miniprep Kit (Qiagen) and insertion of promoter region DNA confirmed with

restriction digestion and gel electroporation. Samples with correct sized inserts were then sent for Sanger Sequencing verification (TAGC, University of Alberta).

3.5 Immunofluorescence Analyses

Immunofluorescence (IF) was used to study frozen sections of human or mouse tissue prepared as above. Tissues were incubated in blocking buffer (0.1% BSA, 0.2% Triton, 5% serum – Goat/Horse, in 1X PBS) for 2hr at room temperature. Which serum blocking buffer is used depends on the choice of secondary antibody selected for detection to prevent the secondary antibody from binding to off-target proteins. After the incubation blocking buffer is removed and the primary antibody is prepared (see Table 3 for list of primary antibodies and dilutions) by dilution in the blocking buffer and left on the tissue overnight at 4°C. Negative controls do not receive a primary antibody, and are left under blocking buffer. The following day slides are rinsed three times for 5 minute intervals with wash solution (1X PBS with 0.05% Triton). The secondary antibody is conjugated to a fluorophore (Table 3), is prepared with the appropriate blocking buffer and placed on the tissue for two hours at room temperature in the dark. After this incubation the samples are again rinsed three times with wash buffer to remove unbound antibody and mounted with Vectashield mounting medium containing DAPI (Vector Labs) under a coverslip. Slides are then sealed with commercial nail polish and stored in the dark at 4°C.

Some samples underwent a modified protocol to achieve dual antibody staining. This protocol is similar to the above, day one being blocking and application of a primary antibody. On the second day, the protocol remains the same until after the incubation and washing of the secondary antibody. Following the wash step the second primary antibody is applied (prepared in the same manner as the first) overnight at 4°C. The next day the tissue is washed 3 fold again, and the secondary antibody to the second primary is applied for 2hr at room temperature. From this point the protocol is the same, with washes followed by mounting with Vectashield.

3.6 Immunohistochemistry Analysis

Immunohistochemistry (IHC) was performed on paraffin embedded tissues provided by collaborators, as well as some frozen sections of mouse tissue taken in the lab. The protocol for

IHC remains similar to IF for both type of tissue; however frozen sections do not need to undergo deparaffinization, rehydration and antigen retrieval.

Formalin-fixed paraffin embedded (FFPE) tissues are baked at 60°C for two hours in an incubator to melt the paraffin wax and expose the tissue. Slides then undergo a series of washes to remove the melted paraffin and rehydrate the tissue for staining. The first series of washes uses Xylene solution for 10 minutes, and then two 2 minute intervals still in Xylene. After this, the slides go through a rehydration gradient of 100% (2x), 95%, 85%, 75% and 50% Ethanol washes for two minute intervals each. This is followed by 5 minutes in ddH₂O. Following rehydration the tissue undergoes antigen retrieval in order to unmask epitopes for antibody binding. 10mM Sodium Citrate buffer (pH 6.0) is brought to a boil in a microwave and the slides are placed into the solution for 30min sitting in room temperature as the solution cools. Any Sodium Citrate remaining after the retrieval is washed off using wash buffer as described in the IF protocol.

From this step onwards frozen sections and FFPE tissues undergo the same treatments. Tissue is placed under the appropriate blocking buffer for 2hrs at room temperature, followed by its removal and replacement with diluted primary antibody. Primary antibody is left on the slides overnight at 4°C. The next day the slides are rinsed 3x in wash buffer for 5 minutes. A biotinylated secondary antibody is prepared and incubated on the slides for two hours at room temperature. Antibodies used, as well as working dilutions can be found in Table 3. After this incubation slides are washed 3x again, and incubated in 0.3% H₂O₂ for 30 minutes. This step blocks endogenous peroxidase activity. After another set of washes the slides are treated with an ABC Solution Kit (Vector Labs) that has been mixed and prepared at room temperature 30 minutes before use. Slides sit under ABC for 30 minutes, and are subsequently washed 3x for 5 min each. During the final wash the DAB chromogenic substrate (Vector Labs) is prepared fresh. It is placed onto the slides for between 1 and 10 minutes, until sufficient stain develops to be visualized. The DAB substrate is then washed off by running the slides under ddH₂O for 5 minutes. At this step; if counterstaining was performed slides are incubated in Meyer's Hematoxylin (Abcam) for 30 seconds. This is followed by a 2 minute wash under running water, and a subsequent 2 minute wash with Scott's Tap water and another 2 minute running water wash. Slides then go through a dehydration gradient (the reverse order of the rehydration

gradient earlier) and are subsequently mounted with Permount Media (Fischer Sciences) and stored at room temperature.

3.8 Electrophoretic Mobility Shift Assay

Electrophoretic Mobility Shift Assays (EMSA) were performed to identify specific homeobox binding motifs that DLX interacts with in the target promoters using an adapted lab protocol (Zhou, Le et al. 2004). Regulatory regions investigated were those identified as interacting with DLX2 from the *in vivo* ChIP experiment. Target regions were amplified from specific segments cloned into the pGL3 plasmid through the use of a Plasmid DNA Maxiprep kit (Qiagen). Regions were excised from the plasmid through restriction digestion using the appropriate restriction enzyme and isolated by gel electrophoresis on a 0.5% agarose gel, and purified using a QIAquick gel extraction kit (Qiagen). These DNA fragments were then 3' radiolabelled on the overhanging base pairs with the Phosphorous – 32 isotope -dNTP (P^{32} -dNTP, Perkin Elmer) and DNA Polymerase I, Large (Klenow) Fragment (NEB) at room temperature for 15 minutes. The reaction was terminated with 1 μ l of 0.5M EDTA and purified with GE Healthcare Illustra Micro-Spin G-25 columns. Radioactivity levels were determined by scintillation counting on a LS 6500 Multi-purpose scintillation counter (Beckman Coulter). Samples for the assay were prepared first by incubating 5x Binding Buffer (Promega) with Poly(dI-dC) at 1mg/ml (a binding competitor) and, 200ng of recombinant DLX2 protein for 30 minutes at room temperature. Following this incubation 100,000 cpm (counts per minute) of radiolabelled probe was added, and incubated for an additional 30 minutes. This preparation is adapted for three distinct controls: (1) the addition of unlabelled probe in excess of 100-fold to labelled to create a Cold Competition sample; (2) a sample lacking recombinant protein to show Free Probe; and (3) the introduction of 2 μ l of DLX2 antibody to induce a Supershift.

A polyacrylamide gel consisting of 40.5ml ddH₂O, 2.5ml 10X Tris/Borate/EDTA (TBE) buffer, 3.125ml 40% (37.5:1) Acrylamide/Bisacrylamide, 1.875ml 40% Acrylamide, 1.56ml 80% Glycerol, 375 μ l 10% Ammonium Persulfate (APS) and 25 μ l Tetramethylethylenediamine (TEMED) was prepared to run the sample mixtures. Prior to loading, the gel was run at 350V for 15 minutes to remove traces of APS remaining in the gel. Once loaded the samples are electrophorated through the gel at 300V for 2 hours in 0.5X TBE buffer. Completed gel runs were

then vacuum/heat dried in a BioRad gel dryer (model 583), and exposed to Kodak autoradiography film for 2 hours at -80°C, followed by film development using a Mini-Medical/90 film processor (AFP Image Works).

3.9 *Luciferase Gene Reporter Assay*

Gene reporter assays were performed on any isolated DNA regions that showed specific *in vitro* interaction with DLX2 in the EMSA assays using a Dual-Luciferase Reporter Assay System (Promega). Regions had been previously cloned into the pGL3 reporter vector (refer to Molecular Cloning) and were prepared for use in this assay. HEK293 cells were chosen for this assay, and were seeded onto T75 cell culture flasks (Fisher Scientific) and grown to confluence in DMEM media (Gibco) + 10% Fetal Bovine Serum (FBS, Fischer) at 37°C, 5% CO₂. At 90% confluence, cells were washed with 1X PBS and subsequently detached from the flask by trypsinization for 3 minutes. This reaction was halted by the addition of DMEM+FBS at the same volume as Trypsin. Cells were collected and counted using a haemocytometer, then diluted to a volume of 175,000 cells/ml of growth media. 1ml of this media was added to each well of a 12 well cell culture plate (Gibco), and incubated for 24 hours prior to transfection. 0.5µg of pGL3 plasmid carrying specific region inserts was then transfected into one column of wells using the Lipofectamine 2000 (Invitrogen) reagent, along with 0.5µg pCDN3-DLX2 expression plasmid. Control wells received 0.5µg empty pGL3 and pCDNA for the respective controls. 6.67 ng pRL-SV40 Renilla vector (Promega) was transformed alongside other plasmids as a control for transfection efficiency. Co-transfected plasmids were incubated in OPTIMEM (Gibco-Invitrogen) while 1µl of transfection reagent was incubated for 5 minutes in an equal amount of OPTIMEM. These two volumes were combined and 100µl of mix was aliquoted per well.

3.10 *Quantitative Reverse Transcription Polymerase Chain Reaction*

To determine the *in vivo* consequences of loss of *Dlx2* on the expression of *Ret*, quantitative reverse transcription PCR (qRT-PCR) was performed on WT and DLX1/2 DKO mouse E13.5 intestinal tissue. Tissue was organized by litter and pup to ensure developing whole intestine,

small intestine (including caecum) and hindgut was taken as per the dissection protocol and flash frozen in liquid nitrogen, then stored at -80°C until genotyping was performed on the pups.

RNA extraction was performed using the TRIzol Reagent (Qiagen) as per the reagent's standard protocol.

cDNA was synthesized from the isolated RNA samples following the Invitrogen Superscript III Reverse Transcriptase Protocol. 500ng of RNA template was combined with 1µl oligo(dT)₂₀ (50 µM), 1µl DNTP mix (10µM) and raised to 13µl total with UltraPure Distilled Water (Invitrogen). This mix was heated at 65°C for 5 minutes followed by placing on wet ice for 1 minute. During the 5 minute heating step a second mix was prepared consisting of 4µl 5X First-Strand Buffer, 1µl DTT (0.1M), 1µl RNaseOUT (40 units/µl) and 1µl Superscript III RT (200units/µl). Following the 1 minute incubation on ice the two mixes were combined and incubated at 50°C for 60 minutes, followed by 70°C for 15 minutes to inactivate the transcriptase reaction.

Quantitative RT-PCR was performed on a Roche LightCycler 96 System using the FastStart Essential DNA Green Master reagent (Roche). *Ret* and *Bmi1* primers (Table 5) were designed to amplify across an exon/exon junction close to the polyA tail to exclude incomplete or degraded cDNA products. The reaction was prepared in a Roche Lightcycler 480 multi well (96) plate, mixing a 20µl reaction containing 5µl PCR grade water (Roche), 10µl Master Mix (Roche), 1µl of each Forward and Reverse Primer (10µM) and 3µl of cDNA template. Each cDNA sample was prepared to 4 technical replicates, with samples from 3 litters comparing WT to DKO within littermates and using a Student's paired T-Test to determine statistical significance. Analysis was performed using Prism7 (GraphPad).

3.11 *Site Directed Mutagenesis*

To determine the specific binding site within target DNA regions containing multiple TAAT/ATTA motifs that were both ChIP and EMSA positive for DLX2 interaction, site directed mutagenesis (SDM) was performed. Primers were designed to alter the binding motif to

eliminate homeodomain binding ability (Table 4) over multiple PCR assays. 3 reactions total were performed to generate mutagenized regions that could be cloned into pGL3 as per the molecular cloning protocol. Two PCR's were performed on gDNA separating the region at the motif into distinct fragments, each reaction altering the nucleotides of the motif individually. This created an overlapping sequence at the 3' and 5' end of the respective products containing the altered binding site. A subsequent reaction was performed using only the forward and reverse primers sets used to add restriction sites to the regions end for cloning. This reaction used a 1:1 mix of mutagenized DNA whose overlapping ends allowed for full amplification of the region while maintaining the altered nucleotides.

Table 1. Primer sets for amplification of ChIP products of *Ret* and *Bmi1* regulatory regions

Gene Region	Forward Primer Sequence	Reverse Primer Sequence
<i>Ret</i> region 1	5'GTCAGAAGGCCTGGAAC	5'GCTAGGAGCCCCTGG
<i>Ret</i> region 2	5'GACCAGGATGGGATTCC	5'CTACGTATGGCCTCTGG
<i>Ret</i> region 3	5'CCAGCCCAAGTCAGCTA	5'GGCTGTCCTCCAGAGTG
<i>Ret</i> region 4	5'CACGGTCATCAGTCAGCTTC	5'CTGATAGGAGCTAAGTTCCAC
<i>Ret</i> region 5	5'CCAGGTCCTAGAGCACTTG	5'CTTCTCTGGGGAAGGTGAG
<i>Ret</i> region 6	5'CTTCCTAGGTGACTCACAG	5'GCATATGCATGCATGCATGC
<i>Ret</i> region 7	5'AGCCACAGGAACCTGTTTG	5'GACATAGGCTGACTTGGGAC
<i>Ret</i> region 8	5'GATTGCTTATTCAACCCTGAG	5'GTTTGCCAGAAGAATCGAAC
<i>Ret</i> region 9	5'TCTCTTTTCATCCTTCCCAAC	5'GTTTGGAGCCTGCAGCTTC
<i>Bmi1</i> region 1	5'CGGGCGTTCAGAGTGTTAAG	5'TGTGGAGACCCAAGGAGTTC
<i>Bmi1</i> region 2	5'GGACAACAAGTATGAAAGTGG	5'GACTGAAAGCAAAGGAGAAAC
<i>Bmi1</i> region 3	5'GTCCATCCAGCAACCACTG	5'CTGGGTCGATCTGTTTCAAG
<i>Bmi1</i> region 4	5'AGGCAGGAAAGCACCAAGT	5'CAGTTTTGCAAACAGCAGGA
<i>Bmi1</i> region 5	5'GGATCCTGACCCAAAATAAAGG	5'AAGCGCCAAGAAACATCAGT
<i>Bmi1</i> region 6	5'ACCGACCTGGATATTTGGTG	5'CTCAAATGCCCACTGAAAGA

<i>Bmi1</i> region 7	5'TTTCAGTGGGCATTTGAGAA	5'TCAGATGCATGATGGAATGAA
<i>Bmi1</i> region 8	5'CATTCCATCATGCATCTGACT	5'GCATATCCATCAATCAACGAA
<i>Bmi1</i> region 9	5'TTCGTTGATTGATGGATATGCT	5'GCTTCTTCTGCTGGATCTGG
<i>Bmi1</i> region 10	5'GATGCTTCAAAAAGCCTGGA	5'GGTTGGCATCACTTCAAAAAGG
<i>Bmi1</i> region 11	5'TGCGTTCCTTCTATCTTGAGC	5'CCTTTCCCGAAACACTTAACCC
<i>Bmi1</i> region 12	5'TGGCGCTGTGGAGAAATG	5'GGAGGGAGGACCAGGAG

Table 2. Primer sets for cloning of ChIP positive regions into pGL3 vector. Restriction sites are highlighted.

Gene	Forward Primer	RE	Reverse Primer	RE
<i>Ret</i> R1	5'TTAGGTACCGTCAGAAGCCTGGAAC	KPN1	5'TTCACGCGTGCTAGGAGCCCACTGG	MLU1
<i>Ret</i> R3	5'TTAGGTACCCAGCCCAAGTCAGCTA	KPN1	5'TCAACGCGTGGCTGTCCTCCAGAGTG	MLU1
<i>Bmi1</i> R1	5'GGTACCTTTCGGGCGTTCAGAGTGTTAAG	KPN1	5'GCTAGCAAATGTGGAGACCCAAGGAGTTC	NHE1
<i>Bmi1</i> R3	5'GGTACCAAAGTCCATCCAGCAACCACTG	KPN1	5'GCTAGCAAACCTGGGTCGATCTGTTCAAG	NHE1
<i>Bmi1</i> R5	5'GGTACCAATGGATCCTGACCCAAAATAA AGG	KPN1	5'GCTAGCAAAAAGCGCCAAGAAACATCAGT	NHE1
<i>Bmi1</i> R9	5'GGTACCACATTTCGTTGATTGATGGATATG CT	KPN1	5'GCTAGCTTTGCTTCTTCTGCTGGATCTGG	NHE1
<i>Bmi1</i> R10	5'GGTACCAAAGATGCTTCAAAAAGCCTGG A	KPN1	5'AAGCTTACAGGTTGGCATCACTTCAAAAAGG	HIND III

Table 3. Antibodies used in immunohistochemical and immunofluorescence analyses of GI tissues.

Antibody	Source	Working Dilution	Primary/ Secondary	Application	Ref. #
Rb polyclonal α -DLX2	De Lab inhouse	1:200	Primary	IHC/IF	N/A
Mouse monoclonal α - Ret	Vector labs	1:100	Primary	IHC/IF	VP-R15L
Rb polyclonal α -PgP 9.5	DAKO	1:1000	Primary	IHC/IF	Z5116
α -Lysozyme	DAKO	1:1000	Primary	IF	A0099
Donkey α - rabbit 488	Life Tech	1:200	Secondary	IF	21206
Donkey α - mouse	Life Tech	1:200	Secondary	IF	A1105

Table 4. Primer sets used for site directed Mutagenesis of *Bmi1* Region 1, altered nucleotides are highlighted

Region	PCR Reaction 1	PCR Reaction 2
<i>Bmi1</i> R1S1	Forward Primer A	Forward Primer C
	5' TTTGGTACCCGGCGCTTCAGAGTGTTAAG	5' CTCAAGTAGGGCGCCTATTGTTTTG
	Reverse Primer B	Reverse Primer D
	5' CAAAACAATAGGCGCCCTACTTGAG	5' AAAGCTAGCTGTGGAGACCCAAGGAGTTC
<i>Bmi1</i> R1S2	Forward Primer A	Forward Primer C
	5' TTTGGTACCCGGCGCTTCAGAGTGTTAAG	5' CGCAGACTGCAATTGTCATCATGGAT
	Reverse Primer B	Reverse Primer D
	5' ATCCATGATGACAATTGCAGTCTGCG	5' AAAGCTAGCTGTGGAGACCCAAGGAGTTC
<i>Bmi1</i> R1S3	Forward Primer A	Forward Primer C
	5' TTTGGTACCCGGCGCTTCAGAGTGTTAAG	5' GCAATGCTATAATGGAGTAAGAGCG
	Reverse Primer B	Reverse Primer D
	5' CGCTCTTACTCCATTATGACAATTGC	5' AAAGCTAGCTGTGGAGACCCAAGGAGTTC
<i>Bmi1</i> R1S4	Forward Primer A	Forward Primer C
	5' TTTGGTACCCGGCGCTTCAGAGTGTTAAG	5' GACAAATCACTTCTAGATGATCCCTC
	Reverse Primer B	Reverse Primer D
	5' GAGGGAATCATCTAGAAGTGATTTGTC	5' AAAGCTAGCTGTGGAGACCCAAGGAGTTC

Table 5. Primers designed for use in RT-PCR experiments.

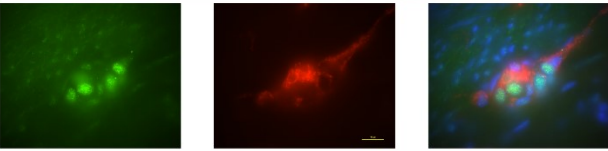
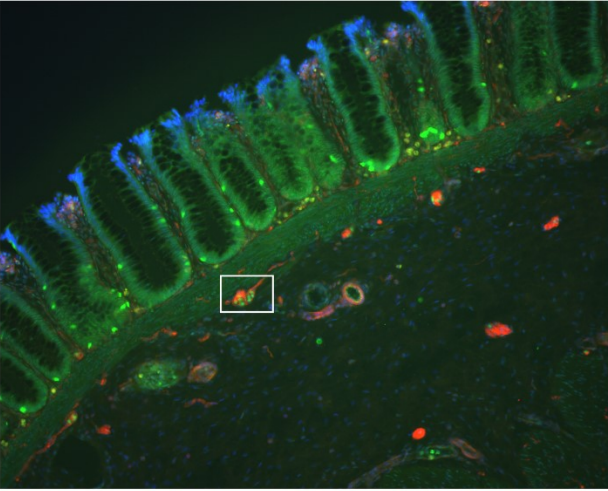
Gene	Forward Primer Sequence	Reverse Primer Sequence
<i>Ret</i>	5' ACTCTATGGCATGTGACACCCG	5' CATTAAATTTGCCGCTGAGGGTG
<i>Bmi1</i>	5' GTCCCAGGGCTTTTCAAAAATGAGATGAAG	5' GTAGTGGGCCATTTCTTCTCCAGG

Chapter 4: *Ret proto-oncogene* regulation by Dlx2: Results

4.1 DLX2 and RET co-expression is observed in a subset of enteric ganglia within ganglionic positive regions of human Hirschsprung's patient intestinal samples.

Co-expression of RET and DLX2 within the ENS was ascertained through double-immunofluorescence assays using antibodies specific to both proteins. Staining was performed on ganglionic segments of cryopreserved human HD tissues to determine co-localization of the two proteins within specific ganglia of the ENS. DLX2 localization is restricted to the nucleus of the cells, while RET can be found in the cytoplasm and cell membrane. Figure 7A shows overlapping expression of DLX2 and RET within ENS cells. A PGP9.5 antibody was used as a general ganglion cell marker in conjunction with the RET antibody to confirm that the cells being seen were specific to the intestinal plexus Figure 7B.

A



B

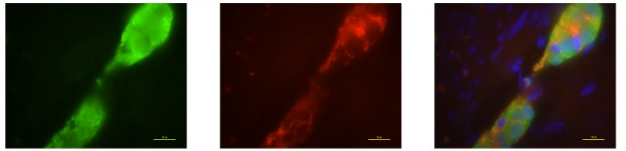
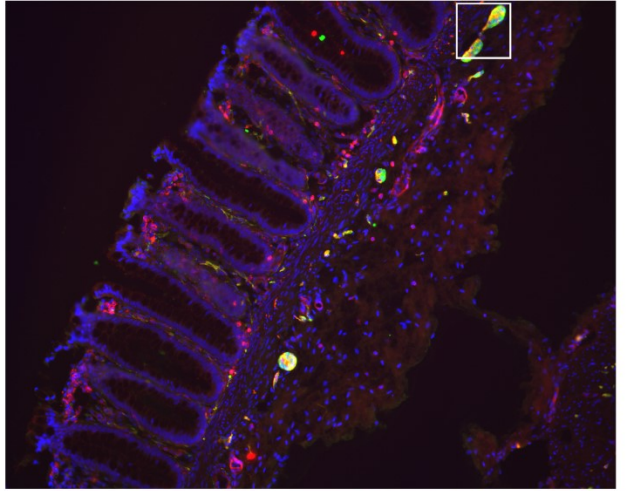


Figure 7. Spatial expression patterns of DLX2 and RET in human HD patient intestinal epithelium and ganglionic intestinal plexus. Dual immunofluorescence assays were performed on sectioned frozen human intestinal tissue to determine which cells express DLX2 and RET, and the co-localization between the two. In all images the blue stain is DAPI. (A) DLX2 (Green) is expressed in specific cells in the intestinal Myenteric Plexus, localized to the nucleus. Staining was performed using a 1:200 dilution of primary antibody. RET (Red) is expressed in a subset of cells expressing DLX2 and localizes to the cell membrane and cytosol. Also note that DLX2 is expressed in the intestinal epithelium, located in enterocytes, enteroendocrine cells and crypts. (B) PGP9.5 (Green) is a ganglion marker that shares a subset of immunostained cells with RET (Red). The differences in co-localization indicate that there are specific ganglia in the ENS that can be distinguished through selective markers, and that DLX2 and RET co-expression may mark specific subsets. Images were taken at 10X magnification, with 40X single/multi-channel images expanded to highlight the overlap in expression.

4.2 *The Ret upstream regulatory region contains multiple homeodomain binding regions.*

DLX2 interacts with the general homeodomain DNA binding motif TAAT/ATTA, 14 of which can be found in the 4KB regulatory region 5' upstream of the RET TSS. As DLX2 has no known consensus binding sequence each of these regions must be considered as a potential binding site. Figure 8 shows the location of each site along the 4kb regulatory region, as well as the division of these regions for subsequent investigations into DLX2 occupancy of the *Ret* promoter. The regulator region has been overlaid with data from the UCSC Genome Browser to provide insight into areas of open and closed chromatin in this region, which will alter the access of DLX2 to the potential binding sites. DNASE1, H3K4 and H3K27Ac are indicators of open chromatin, which corresponds to accessible and active DNA. H3K27me3 is a marker of closed chromatin where transcription is restricted. Each regional division of the regulatory region contains at least one homeodomain binding site and amplifies between 97 and 391 base pairs. Region size was determined through primer optimization and considerations for downstream experiments such as ChIP.

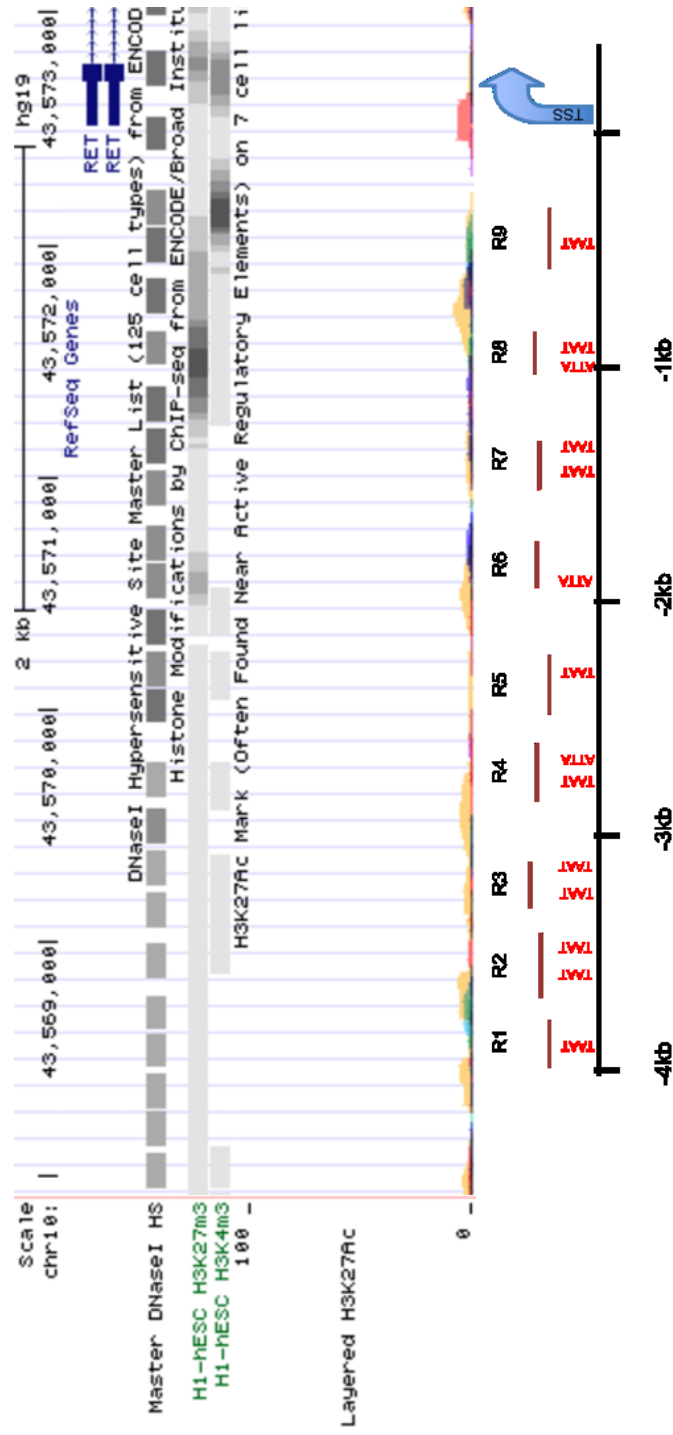


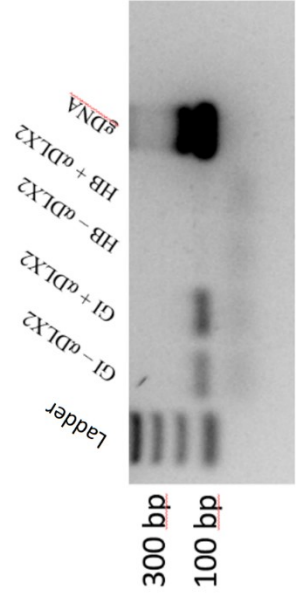
Figure 8. Schematic of 4kb regulatory regions upstream of target gene transcriptional start sites. The *Ret* regulatory region was divided into 10 regions of about 500bps containing 14 TAAT/ATTA motifs upstream of the TSS. The upper figure shows known marks of open and closed chromatin (UCSC genome browser, <http://genome.ucsc.edu>) H3K27me3 marks closed chromatin, open chromatin is marked by DNase1 sensitivity, H3K4me3, and H3K27Ac.

4.3 *DLX2 occupies the Ret promoter in vivo in the mouse model.*

To determine which of the putative binding sites DLX2 occupies in the *Ret* regulatory region ChIP assays were performed on E13 whole intestine. The E13 time-point was selected because at this stage in mouse development the *Ret* driven migration of neural crest derived cells throughout the small and large intestine is completed (Zorn and Wells 2009). Following this migration *Ret* remains active in these cell populations as they begin differentiating. Assays were run on intestinal tissue, as well as hindbrain as a negative tissue control for DLX2 expression, as per the Material and Methods chapter. ChIP enrichment of the *Ret* regulatory regions was verified by PCR analysis, indicating the occupancy of DLX2 in specific regions. Of the nine region divisions, two showed occupancy by DLX2. Regions 1 and 3 show immune enrichment by DLX2 antibody, yielding three potential homeodomain binding sites for subsequent characterization (Figure 9).

E13.5 GI

Ret region 1



Ret region 3

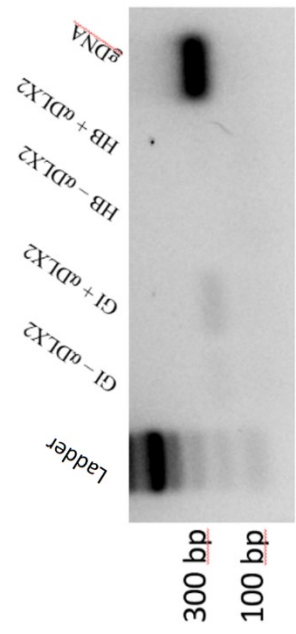




Figure 9. DLX2 occupies specific regulatory regions of *ret in vivo* in the developing mouse gastrointestinal tract. Chromatin immunoprecipitation (ChIP) analysis reveals an interaction between the DLX2 transcription factor and the *Ret* regulatory region *in vivo*. Samples were run on embryonic day 13.5 mouse intestine, with a negative control lacking DLX2 antibody. Additionally, the E13.5 hindbrain is used as a negative tissue control for DLX2 expression. Of the 9 distinct regions containing putative homeodomain binding sites Regions 1 and 3 showed enrichment of DNA in the presence of an anti-DLX2 antibody. The other seven regions were ChIP negative (data not shown).

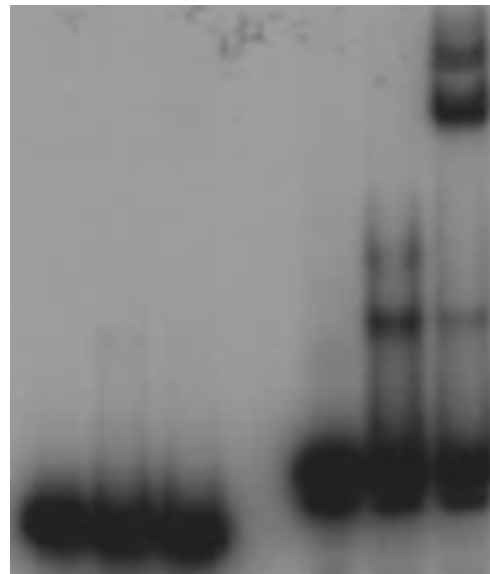
4.4 DLX2 directly binds to the *Ret* regulatory region *in vitro*.

ChIP is a very useful technique for investigating protein:DNA interactions; however it has some limitations. Specificity is an issue in that the ChIP assay can only show occupancy of a binding site by a protein. It shows that the protein of interest is present at the site, but is unable to specify if this interaction is the result of direct or indirect binding. The context of this interaction is very important, as DLX2 could be interacting with the DNA as a member of a complex of proteins. In order to verify whether the interaction shown by ChIP for *Ret* regulatory Regions 1 & 3 is the result of direct binding, Electrophoretic Mobility Shift Assays (EMSA) were performed. Each region was radiolabelled with αP^{32} GTP, and incubated with recombinant DLX2. Regions containing motifs that DLX2 directly binds have a higher molecular weight than those that do not, inducing a gel shift when samples are run on a polyacrylamide gel due to the difference in molecular weight. Figure 10 shows that *Ret* Region 3 is directly bound by DLX2 *in vitro*, while Region 1 is negative, thereby appearing to require additional co-factors for DLX2 interaction. Confirmation of this direct interaction is verified by specifically targeting rDLX2:DNA complexes with a DLX2 antibody, inducing a “supershift” by further increasing the molecular weight of the protein-DNA complex.

Ret region 1

Ret region 3

						
α DLX2	-	-	+	-	-	+
rDLX2	-	+	+	-	+	+
Probe	+	+	+	+	+	+
	1	2	3	4	5	6



← Super Shift

← Specific Shift

← Free Probe

Figure 10. DLX2 directly interacts with *Ret* regulatory region 3 *in vitro*. EMSAs demonstrate specific binding to *Ret* Region 3 (lanes 4-6), but not to Region 1 (1-3). Wells are loaded left to right with radiolabelled free probe DNA fragments (lanes 1,4); labelled probe and recombinant DLX2 (lanes 2, 5); labelled probe, recombinant DLX2 and anti-DLX2 antibody (lanes 3, 6).

4.5 *Dlx2* co-expression significantly inhibits *Ret* reporter gene expression *in vitro*.

ChIP and EMSA assays verified that DLX2 interacts with the *Ret* regulatory region, but do not give any insight into the functional effects of this interaction. Luciferase gene reporter assays were performed *in vitro* to gain an understanding of the significance of *Dlx2* co-expression on *Ret* expression. Region 3 was cloned in to the luciferase expression vector PGL3 and transfected into HEK293 cells alongside either a *Dlx2* pCDNA3 expression vector, or an empty pCDNA vector. HEK293 cells were selected as they contain no detectable endogenous DLX2 expression, as well as for their reliability for use in cell transfections. The functional effect was measured by quantification of the difference in luminescence when the reporter plasmid was transformed with DLX2 or compared to the control (Figure 11). The presence of DLX2 alongside Region 3 resulted in a significant decrease in luciferase expression ($P=0.03$), indicating that DLX2 can have a regulatory effect on *Ret in vitro*. It is important to note that the region studied is a small portion of the regulatory region, and not representative of the total 4 kb segment, as cloning of the large fragment was unsuccessful despite multiple attempts.

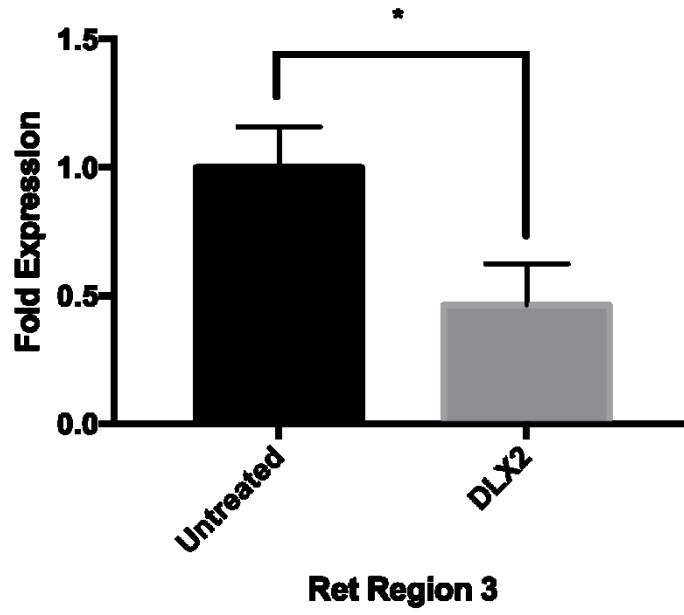


Figure 11. DLX2 restricts *Ret* R3 expression *in vitro*. Luciferase gene reporter assays were performed to determine the potential role of DLX2 expression on the ChIP/EMSA positive *Ret* regulatory region R3. A DLX2 expression vector was transfected into HEK293 cells alongside the *Ret-R3 PGL3* reporter vector and compared to cells co-transfected with the empty expression vector. Results were normalized using internal controls, with transfection efficiency determined by *renilla* expression from the SV40 plasmid. In the presence of DLX2 there was a significant decrease in luciferase expression (P=0.03). The assay was run in triplicate with each run containing three technical replicates of each experimental condition.

4.6 Dlx1/Dlx2 has a significant regulatory effect over Ret in vivo in the developing small and large intestines.

To determine the biological effect of DLX2 on *Ret* expression, semi-quantification of the *Ret* transcript levels was performed on E13 intestinal tissues using quantitative real time PCR. WT and DKO littermates from the *Dlx1/2* DKO mouse line were harvested for RNA extraction and cDNA generation. This assay was performed on both total intestinal tissue and on separated small and large intestine at E13. When examining the whole intestinal tract, spanning both small and large intestine, the absence of both *Dlx1* and *Dlx2* does not appear to have a significant regulatory effect (Figure 12). However, when the assay is performed on isolated small and large intestines, we see significant regulatory differences between the WT and DKO littermates (Figure 13). The small and large intestines were dissected from each other using the cecum to define the start of the large intestine, and then the experiment was repeated on the individual anatomical structures. This subsequent experiment shows that at E13.5 *Ret* expression in the small intestine is significantly ($p = 0.010$) decreased by loss of both *Dlx1* and *Dlx2* gene function (Figure 13A), whereas in the colon we see the opposite effect, where de-repression is occurring in the DKO as seen in Fig. 13B ($p = 0.00080$).

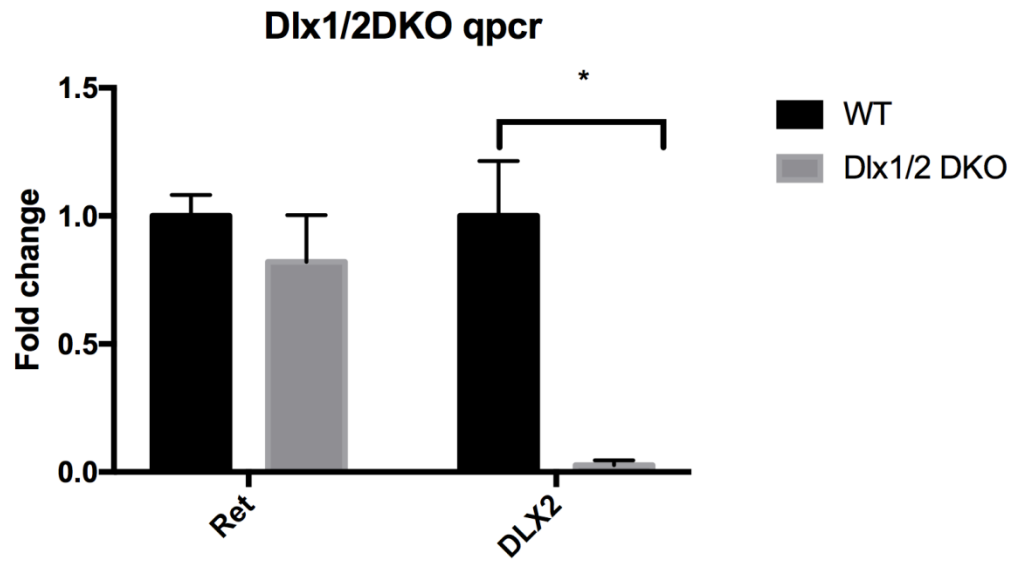


Figure 12. Quantitative real time PCR analysis of the effect that loss of *Dlx1/2* gene function has on *Ret* expression *in vivo*. RNA extracted from whole E13 intestine from *Dlx1/2* DKO and WT littermates was used to make a cDNA library for q-rtPCR analysis. The results were normalized to GAPDH. 4 technical replicates were performed for each sample, with 1 DKO and 1 WT pup samples taken from each of three litters for n=3. To control for genotyping errors, *Dlx2* expression analysis was run alongside and compared to ensure that the DKO pups were not expressing any DLX2.

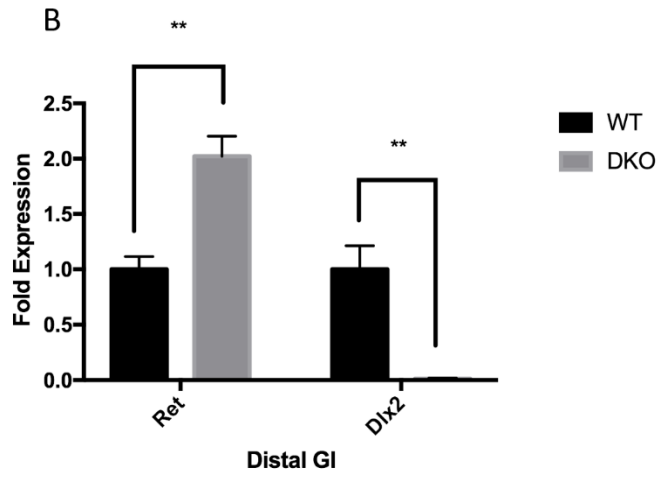
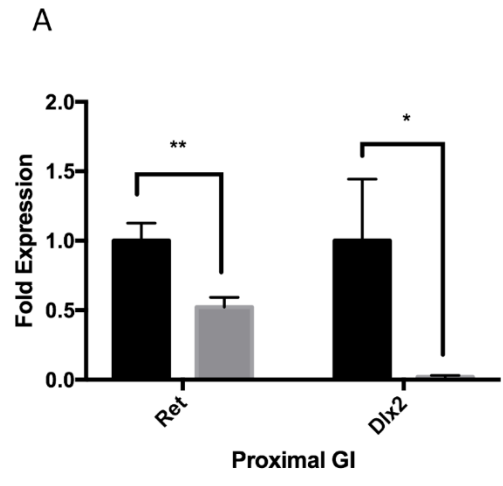


Figure 13. Quantitative PCR of E13 proximal (small intestine) and distal (colon) GIT show significant differences in expression in the absence of *Dlx1/2* gene function. E13 developing intestines were separated into proximal (small) and distal (large) intestinal segments to determine if gene expression alterations were localized to these specific GIT regions. A) qPCR assay run on proximal intestine $p = 0.010$. B) qPCR assay on distal intestine (~2 fold increase), $p = 0.00080$. 4 technical replicates were performed for each sample, with 1 DKO and 1 WT pup samples taken from each of three litters for an $N=3$. To control for genotyping errors, *Dlx2* expression analysis was run alongside and compared to ensure that the DKO pups were not expressing any *Dlx1/2*. Results were normalized using GAPDH as a housekeeping gene.

Chapter 5: *Bmi1* regulation by DLX2: Results

5.1 *DLX2 and Bmi1 co-expression is observed in a subset of cells within the adult mouse intestinal Crypts of Lieberkuhn*

Co-expression of BMI1 and DLX2 within the mouse intestinal tract was performed by Mario Fonseca through double-immunofluorescence assays using antibodies specific to both proteins (Figure 14) (Fonseca and Eisenstat unpublished). Immunofluorescent staining for DLX2 in adult small and large intestines showed its presence in the intestinal crypts (Fig. 14A/B), and further immunostaining using lysozyme revealed the cells expressing DLX2 to be in both Paneth cells and non-Paneth cells of the crypt, indicating that it is present in GIT stem cell populations (Fig. 14C). At the time, *Bmi1* was considered a putative marker of crypt stem cells, and M. Fonseca showed that it was co-expressed in the intestinal crypts with DLX2 (Fig. 14D).

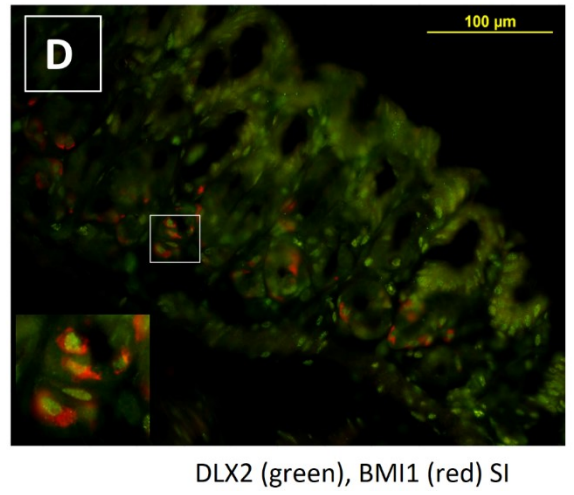
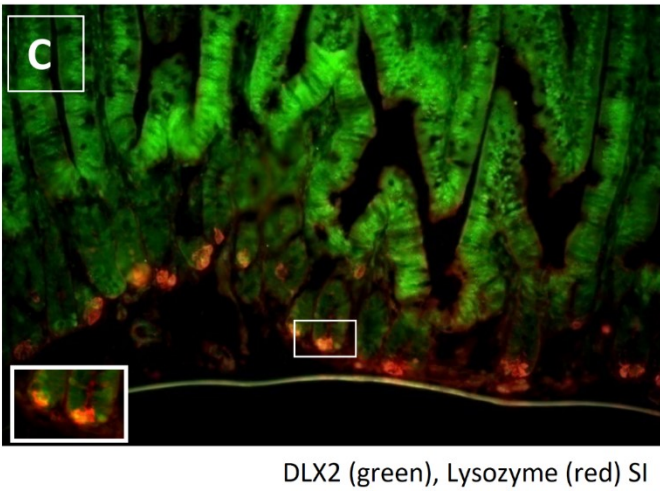
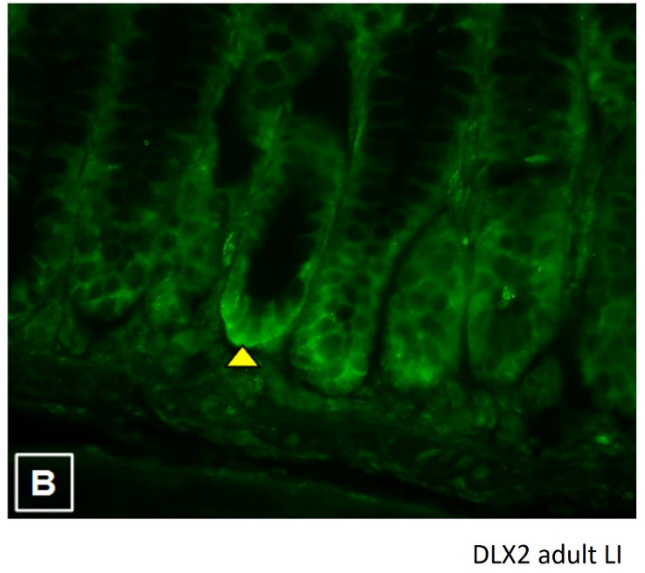
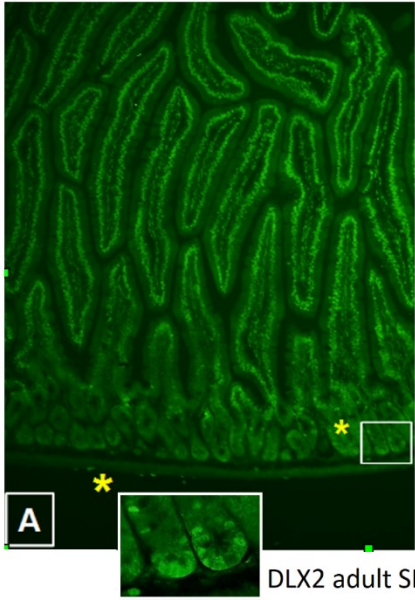


Figure 14. DLX2 is expressed in the cells of the intestinal Crypts of Lieberkuhn and colocalizes with BMI1 in the stem cell populations. A) Adult mouse small intestine shows DLX2 expression (green) in the crypt structures and enterocytes of the epithelium. B) Adult mouse large intestine shows DLX2 expression (green) in the colonocytes and crypt structures of the epithelium. C) DLX2 (green) is observed in some cell populations of the crypt that are distinct from the Paneth cells (red), indicating it is expressed in stem cell. D) DLX2 (green) and BMI1 (Red) colocalize in the stem cells of the crypt niche. Adapted from (Fonseca & Eisenstat, unpublished).

5.2 The *Bmi1* upstream regulatory region contains many homeodomain binding regions

43 homeodomain motifs can be found in the 4KB regulatory region 5' upstream of the *Bmi1* TSS. As DLX2 has no known consensus binding sequence, each of these regions must be considered a potential homeodomain binding site, and so were divided into multiple regions, each spanning a variety of sites. Fig. 15 shows the location of each site along the 4kb regulatory region, as well as the arbitrary division of these regions for investigations into DLX2 occupancy of the *Bmi1* promoter. There are areas of open and closed chromatin in this region, which will alter the access of DLX2 to the potential binding sites, the same marks from the UCSC browser were used as in Figure 8. Each regional division of the regulatory region contains at least one homeodomain binding site and amplifies between 150 and 400 base pairs. Region size was determined through primer optimization and considerations for downstream experiments such as ChIP, as well as the location of binding motifs within each region.

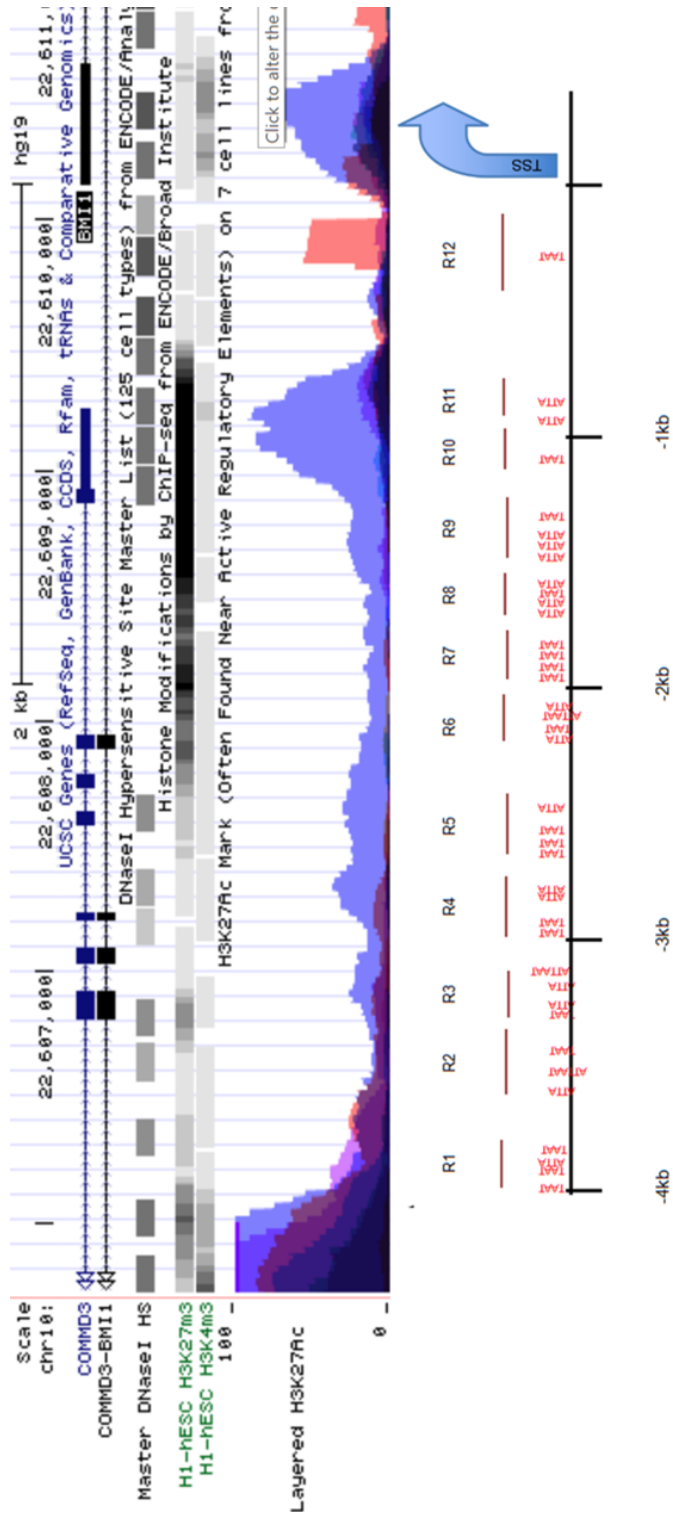


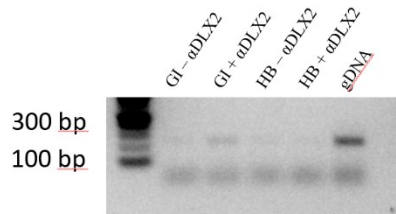
Figure 15. Schematic of 4kb regulatory region upstream of *Bmi1* transcriptional start site.

The *Bmi1* regulatory region divided into 12 regions spanning 43 TAAT/ATTA motifs upstream of the TSS. The upper figure shows known marks of open and closed chromatin (UCSC genome browser, <http://genome.ucsc.edu>) H3K27me3 marks closed chromatin, open chromatin is marked by DNase1 sensitivity, H3K4me3, and H3K27Ac.

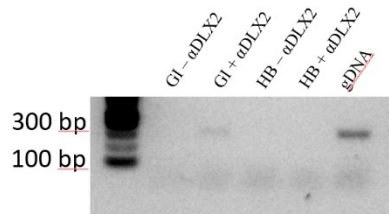
5.3 *DLX2 occupies the Bmi1 promoter in vivo in the mouse model.*

ChIP was performed on E18.5 whole intestine to determine which regions DLX2 interacts with *in vivo*. E18.5 was selected as a time-point due to the structure of the Crypts of Lieberkuhn being fully formed with the stem cell populations present, waiting to be activated (Zorn and Wells 2009). 5 candidate regulatory regions show enrichment for DLX2 after PCR analysis, indicating occupancy at R1, R3, R5, R9 and R10, with a total of 21 putative binding sites. Regions R2, R4, R6, R7, R8 and R11 are ChIP negative and not shown (Figure 16)

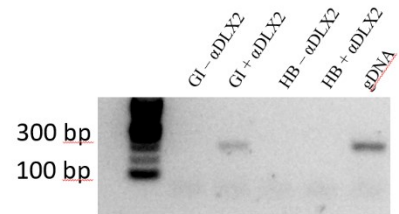
Bmi1 Region 1



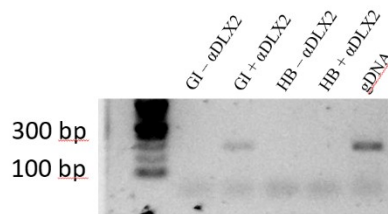
Bmi1 Region 3



Bmi1 Region 5



Bmi1 Region 9



Bmi1 Region 10

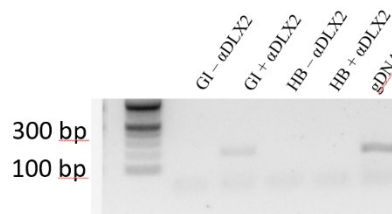


Figure 16. DLX2 occupies specific regulatory regions of *Bmi1* *in vivo* in the developing mouse gastrointestinal tract. Chromatin immunoprecipitation (ChIP) analysis reveals an interaction between the DLX2 transcription factor and the *Bmi1* regulatory region *in vivo*. Samples were run on embryonic day 18.5 mouse intestine, with a negative control lacking DLX2 antibody. Additionally, the E18.5 hindbrain is used as a negative tissue control for DLX2 expression.

5.4 DLX2 directly binds to *Bmi1* regulatory regions *in vitro*.

The limitations to ChIP as described in the *Ret* results section continue to apply. Therefore EMSA assays were performed to determine if DLX2 is directly or indirectly interacting with these *Bmi1* regulatory regions. Figure 17 shows that *Bmi1* Regions 1, 3 and 5 are all directly bound by DLX2 *in vitro*, whereas Regions 9 and 10 showed no gel shifting. This indicates that at least one of the homeodomain binding sites localized to each of R1, 3 and 5 are capable of being directly bound by DLX2. Site directed mutagenesis is a viable method to narrow down which binding site in each region is of importance to DLX2's direct interaction. Figure 18 shows the mutagenesis of the four homeodomain sites in R1, and the reduction of binding when any binding site but R1S1 is deleted.

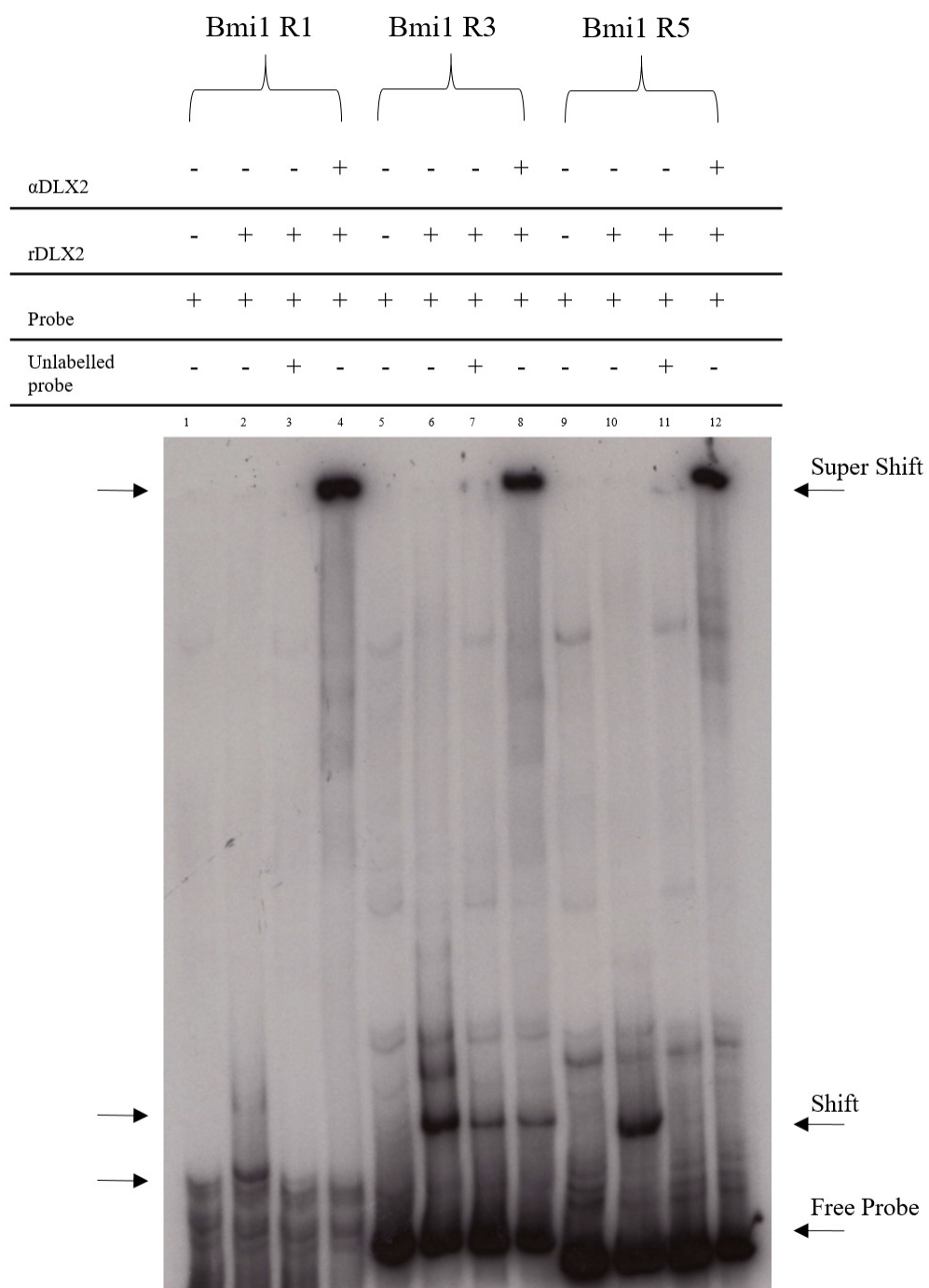


Figure 17. DLX2 directly interacts with *Bmi* regulatory regions 1, 3, and 5 *in vitro*. EMSA demonstrate specific binding to *Bmi1* Regions 1, 3, and 5 (lanes 1-4, 5-8, and 9-12), but not to Regions 9 or 10 (data not shown). Wells are loaded left to right with radiolabelled free probe (lanes 1,5,9); labelled probe and recombinant DLX2 (lanes 2, 6,10); labelled probe, recombinant DLX2 and a 100x excess of unlabelled probe as a competitor (lanes 3, 7, 11) and recombinant DLX2 and a high affinity anti-DLX2 antibody (4, 8, 12).

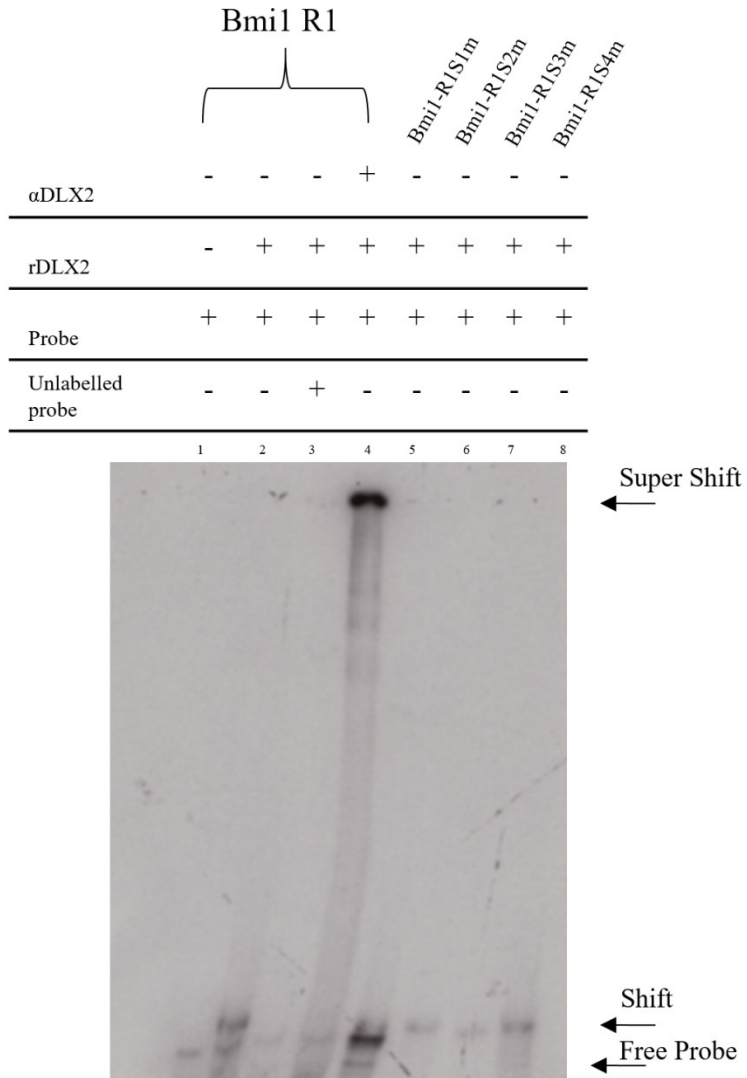
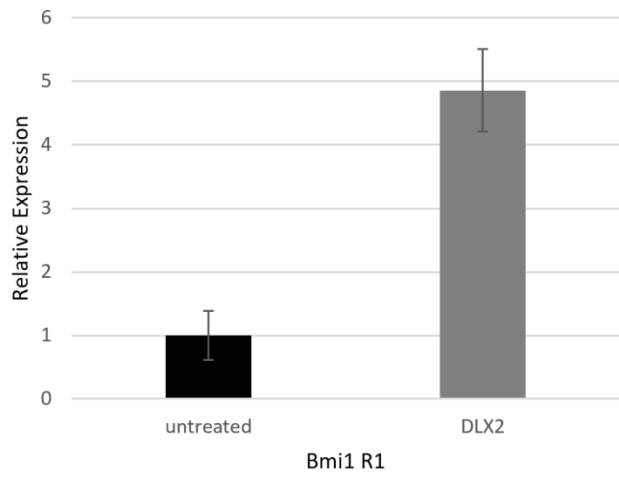


Figure 18. Site directed mutagenesis abolishment of distinct binding sites can determine critical homeodomain motifs for DLX2 binding to *Bmi1 in vitro*. Lanes 1-4 are set up similarly to Figure 15; however, lanes 5-8 used distinct mutagenized probes that had one of the homeodomain binding motifs altered to abolish potential binding. Lane 5 shows that R1S1 was not necessary for induction of a shift in the presence of rDLX2. Lanes 6, 7, and 8 all show reduced shifts resulting from site directed mutagenesis.

5.5 *Dlx2* co-expression significantly activates *Bmi1* Regions 1 & 3 *in vitro*.

Luciferase gene reporter assays were performed to gain an understanding of the effect of DLX2 expression on *Bmi1*. Regions were cloned into the luciferase expression vector pGL3 and transfected into HEK293 cells alongside either *Dlx2* pCDNA3 expression vector, or an empty pCDNA vector. This assay was performed on regulatory regions that showed direct binding from the EMSA assay (R1, R3 & R5). The co-expression of *Dlx2* with Region 3 in Figure 19B resulted in a significant increase in luciferase expression (P= 0.038), indicating that DLX2 can have a positive regulatory effect on *Bmi1 in vitro*. Region 1's results were just short of statistical significance, but show a similar trend as evident for Region 3 (Figure 19A, P= 0.057). Region 5 did not show a significant change in expression when exposed to DLX2 (data not shown).

A



B

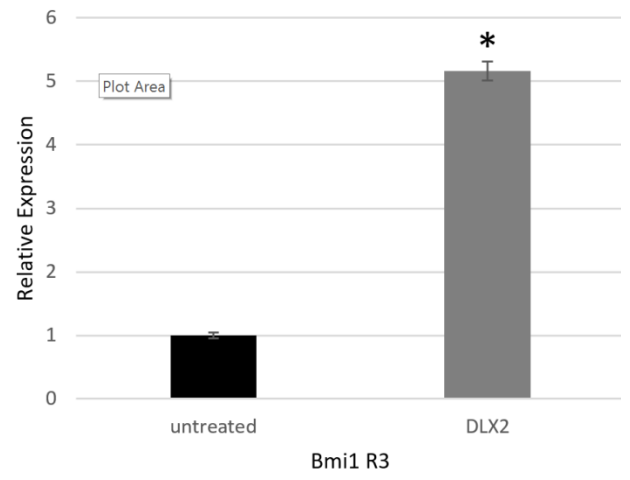


Figure 19. Dlx2 co-expression activates *Bmi1* R3 expression *in vitro*. Luciferase gene reporter assays were performed to determine the role of DLX2 on the ChIP/EMSA positive *Bmi1* regulatory regions (R1 and R3) *in vitro*. A *Dlx2* expression vector was transfected into HEK293 cells alongside the *Bmi1-R1/3/5 PGL3* reporter vectors and compared to cells co-transfected with the empty expression vector. Results were normalized using internal controls, with transfection efficiency determined by *renilla* expression from the SV40 plasmid. A) *Bmi1*-R1 shows high relative activation in the presence of DLX2, (P= 0.057). B) *Bmi1*-R3 shows significant activation in the presence of DLX2 (P= 0.038) that is statistically significant. The assay was run in triplicate with each run containing three technical replicates of each condition.

5.6 *Loss of DLX2 appears to have no effect on Bmi1 expression in the developing mouse intestine in vivo at E18.5 in preliminary experiments.*

To determine the *in vivo* role of DLX2 on *Bmi1*, E18.5 whole intestine was isolated from DKO and WT littermates for investigation using q-rtPCR. This assay is a preliminary investigation as the N= 3 and one more litter is required for analysis. At this developmental time-point, however, we do not see a significant change in *Bmi1* levels in the intestine when *Dlx1/2* expression is lost at this embryonic time-point.

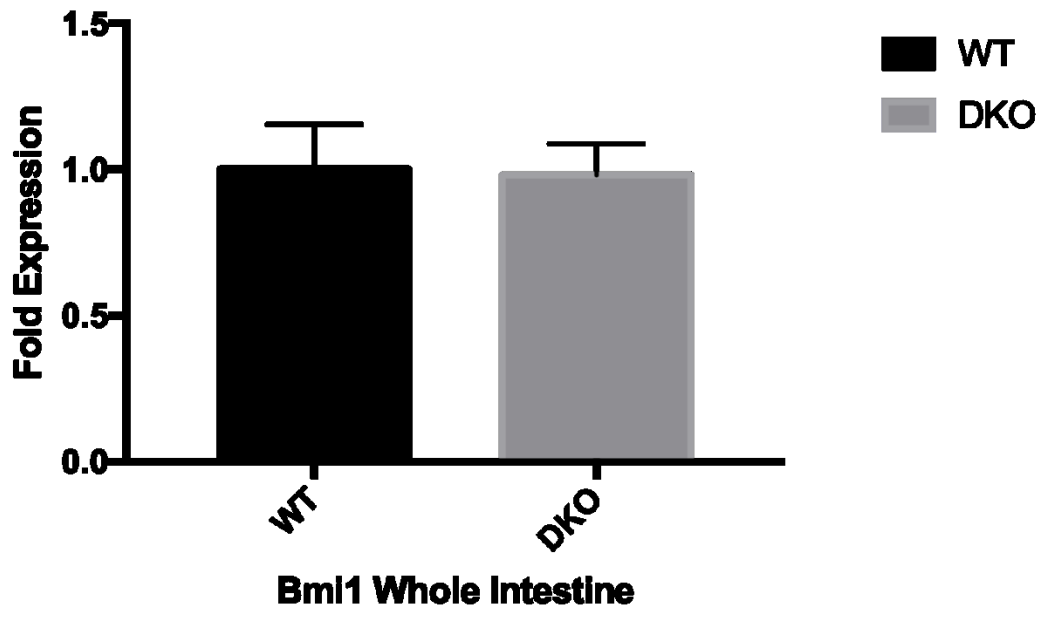


Figure 20. Preliminary qPCR of *Bmi1* expression shows no significant difference upon the loss of *Dlx1/2* gene function. RNA extracted from whole E18.5 Intestine from *Dlx1/2* DKO and WT littermates was used to make a cDNA library for q-rtPCR analysis. The results were normalized to GAPDH. 4 technical replicates were performed for each sample, with 1 DKO and 1 WT pup samples taken from each of two litters for an N=2. One more litter of pups is necessary for this assay to be completed and for proper statistical analysis.

Chapter 6: Discussion

The expression of a gene is a highly controlled and regulated process. Regulation can occur at multiple steps along the pathway of protein generation: (1) at the level of transcription with such methods as transcription factors, chromatin remodelling and enhancers; (2) post-transcriptionally through RNA splicing or micro-RNAs; as well as through (3) translational and post translational means (Solomon, Berg et al. 2002). Homeobox genes are evolutionarily conserved and act as transcriptional regulators of development in a variety of tissues. Proper neuronal, retinal and craniofacial development are all influenced by members of the *Dlx* family genes, with increasing evidence of its role in pancreatic and intestinal development from the Eisenstat lab (Eisenstat, Liu et al. 1999, de Melo, Du et al. 2005, Kraus and Lufkin 2006). This project expanded on the role of *Dlx2* in the developing gastrointestinal tract, looking at its role in neurogenesis of the Enteric Nervous System as well as its function in the regulation of the intestinal Crypt of Lieberkuhn stem cell population, specifically targeting the *Ret proto-oncogene* and *Bmi1* genes, respectively.

6.1 *Dlx2* and *Ret* expression in the developing intestinal tract.

Previous work on the expression of *Dlx2* in the developing mouse has shown its location was restricted to the muscularis propria layer of the intestine until E18.5 when it is also visible in several epithelial cell types (Figure 14, A/B). These early DLX2 positive cells correspond to the Auerbach ganglia (Fonseca and Eisenstat, unpublished). The Auerbach ganglia are Neural Crest Derived Cells (NCDC) found in the myenteric plexus (Figure 1) that are the result of innervation of the intestine (Burns and Douarin 1998). Innervation is a process highly reliant on proper *Ret proto-oncogene* control, a loss of function in which can induce Hirschsprung's disorder due to innervation defects (Asai, Fukuda et al. 2006). The Auerbach ganglia are absent or found at a reduced level in Hirschsprung's patients' distal colon. The initial neonatal presentation of severe HD is a megacolon, a distended intestinal tract caused by proximal blockage (Tam and Garcia-Barcelo 2009). Given this knowledge, as well as the presence of the distended abdomen of the *Dlx1/2* DKO mouse we investigated the co-expression of RET and DLX2 in human intestinal tissues. Figure 7A shows co-expression of RET and DLX2 in ganglia of the human myenteric plexi. This co-localization of protein is a strong indicator that DLX2 could play a role in the regulation of *Ret*, thereby helping to innervate of the intestinal tract. DLX2 is known to be

involved in the central nervous system, helping to control tangential migration of GABAergic interneurons from the ganglionic eminence to the developing neocortex (Anderson, Eisenstat et al. 1997, Le, Du et al. 2007). Both the ENS and the CNS share a common origin in the ectoderm, forming from the neural tube. This common developmental origin combined with the known role of DLX2 in the CNS and the co-expression of DLX2 with RET in the developing ENS is a strong indicator that DLX2 could play an important role in the generation of a subset of the Auerbach ganglia.

6.2 DLX2 directly binds the *Ret* 5' regulatory region during intestinal development

Proper *Ret* regulation is one of the most important parts of intestinal development. Decreased RET can result in a loss of innervation of the lower colon due to a reduction of migrating NCDCs, while RET overexpression results in the development of Multiple Endocrine Neoplasia – type 2 (Mulligan, Kwok et al. 1993). DLX2 is known to directly regulate transcription by binding to homeodomain motifs (ATTA/TAAT) and inducing gene activation such as in *TrkB* in the developing retina or repression as with *Nrp2* in the developing forebrain (Le, Du et al. 2007, de Melo, Zhou et al. 2008). RET expression is maintained throughout the development of the intestine, continuing after innervation is complete, as it is necessary for survival of post-migratory neuronal cells (Uesaka, Nagashimada et al. 2008). To this end, ChIP analysis was performed on mouse E13 whole intestine (large and small combined) as neuronal migration to the distal colon is completed by E12.5, with pan GIT *Ret* expression (Hatch and Mukoyama 2015). Immuno enrichment for DLX2 was seen in two regions of the *Ret* upstream regulatory region, Ret-R1 and Ret-R3, spanning a total of three homeodomain binding sites (Figure 8, Figure 9). This enrichment supports occupation at these two regions by DLX2; it does not, however, tell us the manner of occupation. DLX2 has been known to act on regulatory regions in conjunction with other proteins, such as the MSX1 homeodomain protein, where the two form heterodimeric complexes, although this heterodimerization results in the inhibition of both proteins' transcriptional abilities (Zhang, Hu et al. 1997). To determine if DLX2 is acting directly on the *Ret* regulatory region, mobility shift assays were performed. Figure 10 shows that there is a direct interaction between rDLX2 and Ret-R3 while there is no direct binding of Ret-R1. This indicates that DLX2 could interact with other factors in the regulatory region

encompassed by Ret-R1. Ret-R3 shows direct interaction, but we see multiple bands in the shift and supershift lanes of the EMSA. As there are two distinct bands, and this site encompasses two binding motifs there is a possibility that DLX2 is acting as a homodimer, rather than just a monomeric protein. In order to further explore this consideration, site directed mutagenesis should be performed as discussed in the future directions.

*6.3 Loss of *Dlx1/2* gene function activates *Ret* in the developing small intestine while repressing it in the large intestine at E13.5*

As previously discussed, *Dlx* genes play multiple roles in various developmental and postnatal tissues. In the forebrain they are necessary for interneuron migration, in the retina for cell fate decisions and ganglion cell survival (de Melo, Du et al. 2005, Le, Du et al. 2007, Zhang, Zagozewski et al. 2017). This variability in role based on tissue type complicates working with this transcription factor as each tissue needs to be assessed separately. Having shown that DLX2 directly interacts with the *Ret* regulatory region it is important to determine the effect of this interaction. Maintenance of *Ret* expression is more important in the colon than the small intestine; a study of a conditional knockout line for *Ret* showed that ablation of *Ret* expression post innervation resulted in a near complete loss of colonic ganglion cells, while the small intestine showed no evident loss of ENS cell types (Uesaka, Jain et al. 2007, Uesaka, Nagashimada et al. 2008). This data suggests that Hirschsprung's disorder is not only dependant on *Ret* for innervation, but also for maintenance of those ganglia cells once they have correctly migrated. To determine the role that DLX2 has on *Ret* expression in the developing intestine, quantitative real time PCR was performed on E13.5 tissues comparing WT to *Dlx1/2* DKO. As innervation is completed by E12.5 in the developing mouse GI, by E13.5 *Ret* expression levels should be consistent throughout the compartmentalized structures of the intestinal tract (Pachnis, Mankoo et al. 1993). Using an earlier time-point could complicate results due to a lack of completed innervation in the lower bowel skewing *Ret* expression levels. When we first investigated the effect of loss of *Dlx1/2* gene function on *Ret* within the intestines we isolated cDNA from total intestine of WT and DKO, not separating small from large intestine. This resulted in a non-significant change in expression, trending to a reduction in expression in the DKO samples (Figure 12). When the small and large intestines were separately analyzed we

discovered why we saw no significant change in expression. There appears to be differential regulation of *Ret* expression by DLX2 between the small and large intestine. Interpreting the data, post-innervation the small intestinal *Ret* may be significantly activated in the presence of DLX2, while in the large intestine *Ret* could be repressed by DLX2. This difference in proximal-distal regulation could account for why the whole intestine qrt-PCR yielded a nonsignificant result. Of importance, the *in vitro* gene reporter assay on *Ret*-R3 showed a significant inhibitory effect on the region when *Dlx2* was co-expressed (Figure 13), consistent with what was observed from the large intestine q-rtPCR assay. The difference between small and large intestinal expression of *Ret* could be attributed to the necessity of stricter regulation of its expression in the distal colon. Some possible explanations are that in the developing colon *Ret* is regulated more strictly at the translational level as opposed to the transcriptional level, using protein synthesis and posttranscriptional modifications to have tighter control over RET levels. Alternatively regulation could be less homeostatic in the small intestine as *Ret* appears to be less necessary for neuronal survival in this structure, and therefore does not restrict expression. DLX1 and DLX2 have both been shown to be involved in the proximal/distal regulation of the branchial arches during forebrain development. Mice lacking *Dlx2* or *Dlx1/Dlx2* gene expression present with craniofacial abnormalities due to this regulatory role (Qiu, Bulfone et al. 1995, Qiu, Bulfone et al. 1997). This suggests the potential for other proximal-distal axis roles for DLX driven development.

One possible explanation that is worth investigating further is the number of DLX2 & RET positive ganglia cells found in the large intestine. Preliminary assays on human samples showed co-expression of DLX2 and RET in a subset of Auerbach ganglia (Figure 7A). DLX2 could be inhibiting *Ret* expression in these cells, and upon its loss allowing for increase in *Ret* expression. This finding would indicate that DLX2 is suppressing *Ret* overexpression, thereby reducing the oncogenic properties of *Ret*. This hypothesis would need to be examined *in vitro* through explant studies as the *Dlx1/2* DKO mouse dies at P0 and the adult intestine cannot be examined for signs of Multiple Endocrine Neoplasia type 2. One key limitation is that this hypothesis does not provide a suitable explanation for the distended GI tract of the *Dlx1/2* DKO mouse.

6.4 *Dlx2* directly binds the *Bmi1* regulatory region in the developing intestinal tract

It has been previously established that there is DLX2 expression in the stem cell populations of the intestinal crypts (Figure 14 A-C), (Fonseca and Eisenstat, unpublished) with co-expression of BMI1 at the +4 stem cell position (Figure 14D). At the beginning of this project *Bmi1* was considered as a putative intestinal stem cell marker identifying a quiescent reserve population at the +4 position (Sangiorgi and Capecchi 2008, Yan, Chia et al. 2012). However, subsequent to the start of the project the literature has invalidated *Bmi1* as a stem cell marker, the field preferring *Lgr5* as a marker. Due to its role in regulating cell fate as part of the Polycomb Repressor Complex 1, the project was continued. ChIP analysis of whole E18.5 intestine showed DLX2 immuno-enrichment in multiple regulatory regions containing homeobox binding motifs (Figure 15). *Bmi1*-R1, *Bmi1*-R3, *Bmi1*-R5, *Bmi1*-R9, and *Bmi1*-R10 each showed occupancy by DLX2, spanning a total of 21 putative binding sites (Figure 16). As with the *Ret* ChIP assay, this result does not provide information how DLX2 is interacting with the DNA, so EMSA analysis was performed to determine if binding is direct and specific. Figure 17 shows specific binding of *Bmi1*-R1, R3 & R5, as well as an inducible supershift with a DLX2 antibody. A complication with the homeodomain DNA binding motif rich *Bmi1* regulatory region is that not all of these sites are bound by DLX2 and influence expression. It will therefore be necessary to determine the critical binding sites found in these regulatory regions. This can be determined with a Site Directed Mutagenesis assay where candidate binding motifs are eliminated from the region in such a manner as to narrow down which sites DLX2 binds to *in vitro*. Figure 18 demonstrates this for *Bmi1*-R1. Four mutant vectors of the region were generated, each with a single motif removed. *Bmi1*-R1S1m had a single nucleotide altered in motif site 1 that eliminated the ATTA motif, and showed no loss of DLX2 binding. However, when each of the other sites were removed (*Bmi1*-R1S2m, *Bmi1*-R1S3m, *Bmi1*-R1S4m) a reduction in amount of probe shifted was seen. This indicates that in *Bmi1*-R1 there are multiple motifs that are critical for DLX2 binding *in vitro*. In order to determine exactly which sites are necessary, further SDM experiments must be performed, with alterations in multiple motifs concurrently. An interesting implication of the fact that multiple motifs are involved is that it could indicate that DLX2 regulation requires homodimerization of the protein. DLX2 homodimerization has been described *in vitro* resulting in inhibition of transcriptional activity (Zhang, Hu et al. 1997). An *in vivo* description of the transcriptional effect of dimerized DLX2 would be a valuable next step.

6.5 DLX2 transcriptionally activates *Bmi1* regions *in vitro*

To determine the functional effect of DLX2 interaction with the *Bmi1* regulatory regions an *in vitro* reporter gene assay was performed. Of the three regions that showed direct DLX2 binding only *Bmi1*-R3 showed significant regulatory activation of luciferase reporter expressed *in vitro* (Figure 19B). However, *Bmi1*-R1 shows similar levels of activation with a P-value nearing significance. Together these results support that DLX2 transcriptionally activates *Bmi1 in vivo*. As BMI1 is a member of the PRC1 complex, it is heavily involved in gene silencing through chromatin rearrangement (Gray, Cho et al. 2016). In the intestinal stem cells this is seen in the facultative heterochromatin where the differentiation genes are silenced, until the stem cell divides and begins to differentiate into the four epithelial cell types of the small intestine (Cheng and Leblond 1974, van der Flier and Clevers 2009). Disruption of this essential silencing leads to loss of stem cell renewal as demonstrated by (Molofsky, Pardal et al. 2003) in neuronal stem cells.

The investigation into the biological effect of *Dlx1/Dlx2* on *Bmi1* expression in the developing GIT is underway. A preliminary qPCR on E18.5 whole intestine has been performed with two *Dlx1/2* DKO litters; more litters must be studied to achieve an N of 3. The result of the preliminary assay shows no significant change at this developmental stage (Figure 20). It is possible that *Bmi1* is not functionally a DLX2 target in the developing intestine, although DLX2 has the potential to regulate *Bmi1* transcription *in vitro*. However it is also likely that mice are not an ideal model for this particular assay, as the mouse Crypts of Lieberkuhn do not fully develop until postnatal weeks 3 & 4 (Zorn and Wells 2009). This would complicate the assay as the double knockout mice die at P0, meaning we will not be able to study postnatal DLX2 regulation, which may be occurring in the crypt. A conditional *Dlx2* KO made in the developing intestine could be the solution, as we could look postnatally into late GIT development, as well as observe potential HD or MEN2 phenotypes.

Chapter 7: Conclusions and Future Directions

In this study, we have investigated the role of DLX2 in the developing mouse intestine as a transcriptional regulator of the *Ret proto-oncogene* and the *Bmi1 oncogene*. We have shown that DLX2 occupies the 5' regulatory region of these genes through direct binding of DNA through one or more homeodomain motifs. At E13.5 DLX2 appears to act as an activator of *Ret* in the small intestine and an inhibitor of *Ret* in the large intestine with implications for differential gene regulation along the proximal-distal axis. At E18.5, preliminary results indicate that DLX2 does not regulate *Bmi1* in the intestinal crypts of Lieberkuhn. These results require us to rethink our hypothesis moving forward, as it appears that the role that DLX2 plays in the development of the intestine and ENS is complicated and varied based on developmental age and location.

To bolster our *in vivo* findings for regulation of *Ret* there are some key experiments that should be completed. Characterisation of the *Dlx1/2* DKO intestinal tract through immunohistochemical or *in situ* RNA probes for specific cell types as well as cell cycle and apoptosis analysis should be performed. These assays should be designed to identify the different neuronal cell types of the ENS, and to show if there is a reduction of ENS development in the distal colon. Performing these experiments at multiple embryonic time-points will help to determine the cause of any abnormalities, such as reduced ENS neurons, whether innervation by NCDCs was disrupted or cell death is occurring post innervation. Supplementing this would be semi-quantification of *Ret* expression differences in the small and large intestines at various time-points, as well as investigations into the downstream targets of *Ret* signalling in the *Dlx1/2* DKO mouse.

A limiting factor to these experiments is that the *Dlx1/2* DKO mouse dies on P0. However, a floxed mouse allele for *Dlx2* has recently been generated by the Rubenstein lab (J. Rubenstein, personal communications) so a *cre-lox* system could be created that would allow for inducible tissue specific knockouts. We could therefore investigate postnatal intestinal development, as well as time age specific knockouts of *Dlx2* in the intestine. Another way to work around this limitation is the use of intestinal organoid explants (Grabinger, Luks et al. 2014). Our lab is developing the system to grow and maintain explants *in vitro*, which opens up the possibility of performing knockdowns using siRNA/shRNA or gain of function assays using lentiviral expression vectors transfected into the explants. These offer alternative methods for further investigations without relying on additional genetically engineered mice.

Specific investigations into Hirschsprung's Disorder would also advance the significance of this project and have been planned. Paraffin embedded sections of 19 HD patient intestinal tissue samples have been prepared for immunohistochemical analysis using a variety of ENS neuronal markers. These experiments may indicate what proportion of ganglion cells are DLX2 positive, and how many of them co-express with RET, versus other markers. The FFPE sections span the ganglionic, transition and aganglionic regions of the resected tissue, allowing for analysis into which neuronal cell types are more severely affected by probable loss of *RET* function in the aganglionic region of the samples.

Finally, there exist multiple *Ret* conditional knockout mice that could be brought into the lab for additional studies (Fonseca-Pereira, Arroz-Madeira et al. 2014). These lines could be crossed with the *Dlx1/2* DKO line to generate a triple knockout, or with the CKO *Dlx2* line once it is generated by the lab. Investigations using these mice would allow for research into the biological implications that result from altering the regulatory background of the developing and postnatal intestine.

Many of these future directions apply to the *Bmi1* target as well, such as the use of explant or knockdown technology. One important next step is to investigate the role the loss of *Dlx2* has on postnatal maintenance of the intestinal stem cell populations. To do this we will require the floxed *Dlx2* mouse. Another assay would be to generate organoid cultures of crypts using GFP tagged *Bmi1* expressing cells (Grabinger, Luks et al. 2014). An *in vitro* approach allows for generation of more specific cell types. If DLX2 is only expressed in a subset of intestinal stem cells, *Bmi1* is active throughout the crypts of the small and large intestine, then using whole intestine may be biasing the results. A more specific source of RNA could be consistent with a regulatory effect by *Dlx2*. RNAseq from WT and *Dlx1/2* DKO proximal and distal GIT would be an invaluable source of information for further investigations into the role of *Dlx2* in the developing GIT. Also promising for *Bmi1* is the potential for roles in other tissue types. *Bmi1* expression is widespread throughout different organs, which means the *in vitro* data generated for this target may be applicable to a possible regulatory role for *Dlx2* over *Bmi1* in tissues other than GIT.

Literature Cited:

Alnajar, H., D. Murro, A. Alsadi and S. Jakate (2016). "Spectrum of Clinicopathological Deviations in Long-Segment Hirschsprung Disease Compared With Short-Segment Hirschsprung Disease." Int J Surg Pathol: 1066896916675729.

Amiel, J., E. Sproat-Emison, M. Garcia-Barcelo, F. Lantieri, G. Burzynski, S. Borrego, A. Pelet, S. Arnold, X. Miao, P. Griseri, A. S. Brooks, G. Antinolo, L. de Pontual, M. Clement-Ziza, A. Munnich, C. Kashuk, K. West, K. K. Wong, S. Lyonnet, A. Chakravarti, P. K. Tam, I. Ceccherini, R. M. Hofstra and R. Fernandez (2008). "Hirschsprung disease, associated syndromes and genetics: a review." J Med Genet **45**(1): 1-14.

Anders, J., S. Kjar and C. F. Ibanez (2001). "Molecular modeling of the extracellular domain of the RET receptor tyrosine kinase reveals multiple cadherin-like domains and a calcium-binding site." J Biol Chem **276**(38): 35808-35817.

Anderson, R. B., A. L. Stewart and H. M. Young (2006). "Phenotypes of neural-crest-derived cells in vagal and sacral pathways." Cell Tissue Res **323**(1): 11-25.

Anderson, S. A., D. D. Eisenstat, L. Shi and J. L. Rubenstein (1997). "Interneuron migration from basal forebrain to neocortex: dependence on Dlx genes." Science **278**(5337): 474-476.

Asai, N., T. Fukuda, Z. Wu, A. Enomoto, V. Pachnis, M. Takahashi and F. Costantini (2006). "Targeted mutation of serine 697 in the Ret tyrosine kinase causes migration defect of enteric neural crest cells." Development **133**(22): 4507-4516.

Ayabe, T., D. P. Satchell, C. L. Wilson, W. C. Parks, M. E. Selsted and A. J. Ouellette (2000). "Secretion of microbicidal alpha-defensins by intestinal Paneth cells in response to bacteria." Nat Immunol **1**(2): 113-118.

Badner, J. A., W. K. Sieber, K. L. Garver and A. Chakravarti (1990). "A genetic study of Hirschsprung disease." Am J Hum Genet **46**(3): 568-580.

Barker, N. (2014). "Adult intestinal stem cells: critical drivers of epithelial homeostasis and regeneration." Nat Rev Mol Cell Biol **15**(1): 19-33.

Barker, N., J. H. van Es, J. Kuipers, P. Kujala, M. van den Born, M. Cozijnsen, A. Haegebarth, J. Korving, H. Begthel, P. J. Peters and H. Clevers (2007). "Identification of stem cells in small intestine and colon by marker gene Lgr5." Nature **449**(7165): 1003-1007.

Barlow, A., E. de Graaff and V. Pachnis (2003). "Enteric nervous system progenitors are coordinately controlled by the G protein-coupled receptor EDNRB and the receptor tyrosine kinase RET." Neuron **40**(5): 905-916.

Bowles, J., G. Schepers and P. Koopman (2000). "Phylogeny of the SOX family of developmental transcription factors based on sequence and structural indicators." Dev Biol **227**(2): 239-255.

Bradnock, T. J., M. Knight, S. Kenny, M. Nair and G. M. Walker (2017). "Hirschsprung's disease in the UK and Ireland: incidence and anomalies." Arch Dis Child.

Burns, A. J. and N. M. Douarin (1998). "The sacral neural crest contributes neurons and glia to the post-umbilical gut: spatiotemporal analysis of the development of the enteric nervous system." Development **125**(21): 4335-4347.

Cao, R., L. Wang, H. Wang, L. Xia, H. Erdjument-Bromage, P. Tempst, R. S. Jones and Y. Zhang (2002). "Role of histone H3 lysine 27 methylation in Polycomb-group silencing." Science **298**(5595): 1039-1043.

Carrasco, A. E., W. McGinnis, W. J. Gehring and E. M. De Robertis (1984). "Cloning of an X. laevis gene expressed during early embryogenesis coding for a peptide region homologous to Drosophila homeotic genes." Cell **37**(2): 409-414.

Chang, W. W. and C. P. Leblond (1971). "Renewal of the epithelium in the descending colon of the mouse. I. Presence of three cell populations: vacuolated-columnar, mucous and argentaffin." Am J Anat **131**(1): 73-99.

Cheng, H. and C. P. Leblond (1974). "Origin, differentiation and renewal of the four main epithelial cell types in the mouse small intestine. V. Unitarian Theory of the origin of the four epithelial cell types." Am J Anat **141**(4): 537-561.

Cranston, A., C. Carniti, S. Martin, P. Mondellini, Y. Hooks, J. Leyland, S. Hodgson, S. Clarke, M. Pierotti, B. A. Ponder and I. Bongarzone (2006). "A novel activating mutation in the RET tyrosine kinase domain mediates neoplastic transformation." Mol Endocrinol **20**(7): 1633-1643.

de Lau, W., W. C. Peng, P. Gros and H. Clevers (2014). "The R-spondin/Lgr5/Rnf43 module: regulator of Wnt signal strength." Genes Dev **28**(4): 305-316.

de Melo, J., G. Du, M. Fonseca, L. A. Gillespie, W. J. Turk, J. L. Rubenstein and D. D. Eisenstat (2005). "Dlx1 and Dlx2 function is necessary for terminal differentiation and survival of late-born retinal ganglion cells in the developing mouse retina." Development **132**(2): 311-322.

de Melo, J., Q. P. Zhou, Q. Zhang, S. Zhang, M. Fonseca, J. T. Wigle and D. D. Eisenstat (2008). "Dlx2 homeobox gene transcriptional regulation of Trkb neurotrophin receptor expression during mouse retinal development." Nucleic Acids Res **36**(3): 872-884.

de Vries, P. A. and G. W. Friedland (1974). "The staged sequential development of the anus and rectum in human embryos and fetuses." J Pediatr Surg **9**(5): 755-769.

Du, F. and S. Liu (2015). "Electroacupuncture with high frequency at acupoint ST-36 induces regeneration of lost enteric neurons in diabetic rats via GDNF and PI3K/AKT signal pathway." Am J Physiol Regul Integr Comp Physiol **309**(2): R109-118.

Du, F., L. Wang, W. Qian and S. Liu (2009). "Loss of enteric neurons accompanied by decreased expression of GDNF and PI3K/Akt pathway in diabetic rats." Neurogastroenterol Motil **21**(11): 1229-e1114.

Eisenstat, D. D., J. K. Liu, M. Mione, W. Zhong, G. Yu, S. A. Anderson, I. Ghattas, L. Puelles and J. L. Rubenstein (1999). "DLX-1, DLX-2, and DLX-5 expression define distinct stages of basal forebrain differentiation." J Comp Neurol **414**(2): 217-237.

Eng, C., D. Clayton, I. Schuffenecker, G. Lenoir, G. Cote, R. F. Gagel, H. K. van Amstel, C. J. Lips, I. Nishisho, S. I. Takai, D. J. Marsh, B. G. Robinson, K. Frank-Raue, F. Raue, F. Xue, W. W. Noll, C. Romei, F. Pacini, M. Fink, B. Niederle, J. Zedenius, M. Nordenskjold, P. Komminoth, G. N. Hendy, L. M. Mulligan and et al. (1996). "The relationship between specific RET proto-oncogene mutations and disease phenotype in multiple endocrine neoplasia type 2. International RET mutation consortium analysis." Jama **276**(19): 1575-1579.

Farcas, A. M., N. P. Blackledge, I. Sudbery, H. K. Long, J. F. McGouran, N. R. Rose, S. Lee, D. Sims, A. Cerase, T. W. Sheahan, H. Koseki, N. Brockdorff, C. P. Ponting, B. M. Kessler and R. J. Klose (2012). "KDM2B links the Polycomb Repressive Complex 1 (PRC1) to recognition of CpG islands." Elife **1**: e00205.

Fonseca-Pereira, D., S. Arroz-Madeira, M. Rodrigues-Campos, I. A. Barbosa, R. G. Domingues, T. Bento, A. R. Almeida, H. Ribeiro, A. J. Potocnik, H. Enomoto and H. Veiga-Fernandes (2014). "The neurotrophic factor receptor RET drives haematopoietic stem cell survival and function." Nature **514**(7520): 98-101.

Formeister, E. J., A. L. Sionas, D. K. Lorance, C. L. Barkley, G. H. Lee and S. T. Magness (2009). "Distinct SOX9 levels differentially mark stem/progenitor populations and enteroendocrine cells of the small intestine epithelium." Am J Physiol Gastrointest Liver Physiol **296**(5): G1108-1118.

Fu, M., Y. Sato, A. Lyons-Warren, B. Zhang, M. A. Kane, J. L. Napoli and R. O. Heuckeroth (2010). "Vitamin A facilitates enteric nervous system precursor migration by reducing Pten accumulation." Development **137**(4): 631-640.

Furness, J. B. (2000). "Types of neurons in the enteric nervous system." J Auton Nerv Syst **81**(1-3): 87-96.

Gabriel, S. B., R. Salomon, A. Pelet, M. Angrist, J. Amiel, M. Fornage, T. Attie-Bitach, J. M. Olson, R. Hofstra, C. Buys, J. Steffann, A. Munnich, S. Lyonnet and A. Chakravarti (2002). "Segregation at three loci explains familial and population risk in Hirschsprung disease." Nat Genet **31**(1): 89-93.

Gao, Z., J. Zhang, R. Bonasio, F. Strino, A. Sawai, F. Parisi, Y. Kluger and D. Reinberg (2012). "PCGF homologs, CBX proteins, and RYBP define functionally distinct PRC1 family complexes." Mol Cell **45**(3): 344-356.

Gebert, A., H. J. Rothkotter and R. Pabst (1996). "M cells in Peyer's patches of the intestine." Int Rev Cytol **167**: 91-159.

Grabinger, T., L. Luks, F. Kostadinova, C. Zimmerlin, J. P. Medema, M. Leist and T. Brunner (2014). "Ex vivo culture of intestinal crypt organoids as a model system for assessing cell death induction in intestinal epithelial cells and enteropathy." Cell Death Dis **5**: e1228.

Gray, F., H. J. Cho, S. Shukla, S. He, A. Harris, B. Boytsov, L. Jaremko, M. Jaremko, B. Demeler, E. R. Lawlor, J. Grembecka and T. Cierpicki (2016). "BMI1 regulates PRC1 architecture and activity through homo- and hetero-oligomerization." Nat Commun **7**: 13343.

Gribble, F. M. and F. Reimann (2016). "Enteroendocrine Cells: Chemosensors in the Intestinal Epithelium." Annu Rev Physiol **78**: 277-299.

Gujral, T. S., V. K. Singh, Z. Jia and L. M. Mulligan (2006). "Molecular mechanisms of RET receptor-mediated oncogenesis in multiple endocrine neoplasia 2B." Cancer Res **66**(22): 10741-10749.

Hatch, J. and Y. S. Mukoyama (2015). "Spatiotemporal mapping of vascularization and innervation in the fetal murine intestine." Dev Dyn **244**(1): 56-68.

Heath, J. K. (2010). "Transcriptional networks and signaling pathways that govern vertebrate intestinal development." Curr Top Dev Biol **90**: 159-192.

Hofer, D. and D. Drenckhahn (1996). "Cytoskeletal markers allowing discrimination between brush cells and other epithelial cells of the gut including enteroendocrine cells." Histochem Cell Biol **105**(5): 405-412.

Hofstra, R. M., Y. Wu, R. P. Stulp, P. Elfferich, J. Osinga, S. M. Maas, L. Siderius, A. S. Brooks, J. J. vd Ende, V. M. Heydendaal, R. S. Severijnen, K. M. Bax, C. Meijers and C. H. Buys (2000). "RET and GDNF gene scanning in Hirschsprung patients using two dual denaturing gel systems." Hum Mutat **15**(5): 418-429.

Inabnet, W. B., P. Caragliano and D. Pertsemlidis (2000). "Pheochromocytoma: inherited associations, bilaterality, and cortex preservation." Surgery **128**(6): 1007-1011;discussion 1011-1002.

Jing, S., D. Wen, Y. Yu, P. L. Holst, Y. Luo, M. Fang, R. Tamir, L. Antonio, Z. Hu, R. Cupples, J. C. Louis, S. Hu, B. W. Altmann and G. M. Fox (1996). "GDNF-induced activation of the ret protein tyrosine kinase is mediated by GDNFR-alpha, a novel receptor for GDNF." Cell **85**(7): 1113-1124.

Kashuk, C. S., E. A. Stone, E. A. Grice, M. E. Portnoy, E. D. Green, A. Sidow, A. Chakravarti and A. S. McCallion (2005). "Phenotype-genotype correlation in Hirschsprung disease is illuminated by comparative analysis of the RET protein sequence." Proc Natl Acad Sci U S A **102**(25): 8949-8954.

Kawamoto, Y., K. Takeda, Y. Okuno, Y. Yamakawa, Y. Ito, R. Taguchi, M. Kato, H. Suzuki, M. Takahashi and I. Nakashima (2004). "Identification of RET autophosphorylation sites by mass spectrometry." J Biol Chem **279**(14): 14213-14224.

Kraus, P. and T. Lufkin (2006). "Dlx homeobox gene control of mammalian limb and craniofacial development." Am J Med Genet A **140**(13): 1366-1374.

Kuzmichev, A., K. Nishioka, H. Erdjument-Bromage, P. Tempst and D. Reinberg (2002). "Histone methyltransferase activity associated with a human multiprotein complex containing the Enhancer of Zeste protein." Genes Dev **16**(22): 2893-2905.

Latorre, R., C. Sternini, R. De Giorgio and B. Greenwood-Van Meerveld (2016). "Enteroendocrine cells: a review of their role in brain-gut communication." Neurogastroenterol Motil **28**(5): 620-630.

Le, T. N., G. Du, M. Fonseca, Q. P. Zhou, J. T. Wigle and D. D. Eisenstat (2007). "Dlx homeobox genes promote cortical interneuron migration from the basal forebrain by direct repression of the semaphorin receptor neuropilin-2." J Biol Chem **282**(26): 19071-19081.

Leon, T. Y., E. S. Ngan, H. C. Poon, M. T. So, V. C. Lui, P. K. Tam and M. M. Garcia-Barcelo (2009). "Transcriptional regulation of RET by Nkx2-1, Phox2b, Sox10, and Pax3." J Pediatr Surg **44**(10): 1904-1912.

Li, Y., T. Kido, M. M. Garcia-Barcelo, P. K. Tam, Z. L. Tabatabai and Y. F. Lau (2015). "SRY interference of normal regulation of the RET gene suggests a potential role of the Y-chromosome gene in sexual dimorphism in Hirschsprung disease." Hum Mol Genet **24**(3): 685-697.

Madara, J. L. (1982). "Cup cells: structure and distribution of a unique class of epithelial cells in guinea pig, rabbit, and monkey small intestine." Gastroenterology **83**(5): 981-994.

Mahmoudi, T. and C. P. Verrijzer (2001). "Chromatin silencing and activation by Polycomb and trithorax group proteins." Oncogene **20**(24): 3055-3066.

Margueron, R. and D. Reinberg (2011). "The Polycomb complex PRC2 and its mark in life." Nature **469**(7330): 343-349.

Marquard, J. and C. Eng (1993). Multiple Endocrine Neoplasia Type 2. GeneReviews(R). R. A. Pagon, M. P. Adam, H. H. Ardinger et al. Seattle (WA), University of Washington, Seattle University of Washington, Seattle. GeneReviews is a registered trademark of the University of Washington, Seattle. All rights reserved.

McGuinness, T., M. H. Porteus, S. Smiga, A. Bulfone, C. Kingsley, M. Qiu, J. K. Liu, J. E. Long, D. Xu and J. L. Rubenstein (1996). "Sequence, organization, and transcription of the Dlx-1 and Dlx-2 locus." Genomics **35**(3): 473-485.

Metzger, M., C. Caldwell, A. J. Barlow, A. J. Burns and N. Thapar (2009). "Enteric nervous system stem cells derived from human gut mucosa for the treatment of aganglionic gut disorders." Gastroenterology **136**(7): 2214-2225.e2211-2213.

Mochizuki, K., M. Shinkai, N. Kitagawa, H. Take, H. Usui, T. Hosokawa and K. Yamoto (2017). "Continuous transanal decompression for infants with long- and total-type Hirschsprung's diseases as a bridge to curative surgery: a single-center experience." Surg Case Rep **3**(1): 42.

Molofsky, A. V., R. Pardal, T. Iwashita, I. K. Park, M. F. Clarke and S. J. Morrison (2003). "Bmi-1 dependence distinguishes neural stem cell self-renewal from progenitor proliferation." Nature **425**(6961): 962-967.

Montgomery, R. K., D. L. Carlone, C. A. Richmond, L. Farilla, M. E. Kranendonk, D. E. Henderson, N. Y. Baffour-Awuah, D. M. Ambruzs, L. K. Fogli, S. Algra and D. T. Breault (2011). "Mouse telomerase reverse transcriptase (mTert) expression marks slowly cycling intestinal stem cells." Proc Natl Acad Sci U S A **108**(1): 179-184.

Montgomery, R. K., A. E. Mulberg and R. J. Grand (1999). "Development of the human gastrointestinal tract: twenty years of progress." Gastroenterology **116**(3): 702-731.

Moore, S. W. (2016). "Advances in understanding functional variations in the Hirschsprung disease spectrum (variant Hirschsprung disease)." Pediatr Surg Int.

Mulligan, L. M., J. B. Kwok, C. S. Healey, M. J. Elsdon, C. Eng, E. Gardner, D. R. Love, S. E. Mole, J. K. Moore, L. Papi and et al. (1993). "Germ-line mutations of the RET proto-oncogene in multiple endocrine neoplasia type 2A." Nature **363**(6428): 458-460.

Mwizerwa, O., P. Das, N. Nagy, S. E. Akbareian, J. D. Mably and A. M. Goldstein (2011). "Gdnf is mitogenic, neurotrophic, and chemoattractive to enteric neural crest cells in the embryonic colon." Dev Dyn **240**(6): 1402-1411.

Nagy, N. and A. M. Goldstein (2006). "Endothelin-3 regulates neural crest cell proliferation and differentiation in the hindgut enteric nervous system." Dev Biol **293**(1): 203-217.

Nagy, N. and A. M. Goldstein (2017). "Enteric nervous system development: A crest cell's journey from neural tube to colon." Semin Cell Dev Biol.

Nakagawa, T., T. Kajitani, S. Togo, N. Masuko, H. Ohdan, Y. Hishikawa, T. Koji, T. Matsuyama, T. Ikura, M. Muramatsu and T. Ito (2008). "Deubiquitylation of histone H2A activates transcriptional initiation via trans-histone cross-talk with H3K4 di- and trimethylation." Genes Dev **22**(1): 37-49.

Pachnis, V., B. Mankoo and F. Costantini (1993). "Expression of the c-ret proto-oncogene during mouse embryogenesis." Development **119**(4): 1005-1017.

Pansky, B. (1982). Review of Medical Embryology, McGraw-Hill.

Potten, C. S. (1998). "Stem cells in gastrointestinal epithelium: numbers, characteristics and death." Philos Trans R Soc Lond B Biol Sci **353**(1370): 821-830.

Powell, A. E., Y. Wang, Y. Li, E. J. Poulin, A. L. Means, M. K. Washington, J. N. Higginbotham, A. Juchheim, N. Prasad, S. E. Levy, Y. Guo, Y. Shyr, B. J. Aronow, K. M. Haigis, J. L. Franklin and R. J. Coffey (2012). "The pan-ErbB negative regulator Lrig1 is an intestinal stem cell marker that functions as a tumor suppressor." Cell **149**(1): 146-158.

Qiu, M., A. Bulfone, I. Ghattas, J. J. Meneses, L. Christensen, P. T. Sharpe, R. Presley, R. A. Pedersen and J. L. Rubenstein (1997). "Role of the Dlx homeobox genes in proximodistal patterning of the branchial arches: mutations of Dlx-1, Dlx-2, and Dlx-1 and -2 alter morphogenesis of proximal skeletal and soft tissue structures derived from the first and second arches." Dev Biol **185**(2): 165-184.

Qiu, M., A. Bulfone, S. Martinez, J. J. Meneses, K. Shimamura, R. A. Pedersen and J. L. Rubenstein (1995). "Null mutation of Dlx-2 results in abnormal morphogenesis of proximal first and second branchial arch derivatives and abnormal differentiation in the forebrain." Genes Dev **9**(20): 2523-2538.

Reid, L., B. Meyrick, V. B. Antony, L. Y. Chang, J. D. Crapo and H. Y. Reynolds (2005). "The mysterious pulmonary brush cell: a cell in search of a function." Am J Respir Crit Care Med **172**(1): 136-139.

- Richmond, C. A., M. S. Shah, D. L. Carlone and D. T. Breault (2016). "An enduring role for quiescent stem cells." Dev Dyn **245**(7): 718-726.
- Sadler, T. W. and J. Langman (2012). Langman's medical embryology. Philadelphia, Wolters Kluwer Health/Lippincott Williams & Wilkins.
- Sancho, E., E. Batlle and H. Clevers (2003). "Live and let die in the intestinal epithelium." Curr Opin Cell Biol **15**(6): 763-770.
- Sandle, G. I. (1998). "Salt and water absorption in the human colon: a modern appraisal." Gut **43**(2): 294-299.
- Sangiorgi, E. and M. R. Capecchi (2008). "Bmi1 is expressed in vivo in intestinal stem cells." Nat Genet **40**(7): 915-920.
- Schriemer, D., Y. Sribudiani, I. J. A. D. Natarajan, K. C. MacKenzie, M. Metzger, E. Binder, A. J. Burns, N. Thapar, R. M. Hofstra and B. J. Eggen (2016). "Regulators of gene expression in Enteric Neural Crest Cells are putative Hirschsprung disease genes." Dev Biol **416**(1): 255-265.
- Sergi, C. M., O. Caluseriu, H. McColl and D. D. Eisenstat (2017). "Hirschsprung's disease: clinical dysmorphology, genes, micro-RNAs, and future perspectives." Pediatr Res **81**(1-2): 177-191.
- Shaker, A. and D. C. Rubin (2010). "Intestinal stem cells and epithelial-mesenchymal interactions in the crypt and stem cell niche." Transl Res **156**(3): 180-187.
- Sheng, G., E. Harris, C. Bertuccioli and C. Desplan (1997). "Modular organization of Pax/homeodomain proteins in transcriptional regulation." Biol Chem **378**(8): 863-872.
- Simkin, J. E., D. Zhang, B. N. Rollo and D. F. Newgreen (2013). "Retinoic acid upregulates ret and induces chain migration and population expansion in vagal neural crest cells to colonise the embryonic gut." PLoS One **8**(5): e64077.
- Snoeck, V., B. Goddeeris and E. Cox (2005). "The role of enterocytes in the intestinal barrier function and antigen uptake." Microbes Infect **7**(7-8): 997-1004.
- Solomon, E. P., L. R. Berg and D. W. Martin (2002). Biology, Brooks/Cole Thomson Learning.
- Soroa-Ruiz, F., H. Lara-Sanchez, J. Ramirez Anguiano and J. C. Cordova-Ramon (2014). "[Multiple mucosal neuromas in the larynx as part of a multiple endocrine neoplasia type 2B]." Acta Otorrinolaringol Esp **65**(3): 197-199.

Stanfel, M. N., K. A. Moses, R. J. Schwartz and W. E. Zimmer (2005). "Regulation of organ development by the NKX-homeodomain factors: an NKX code." Cell Mol Biol (Noisy-le-grand) Suppl **51**: O1785-799.

Stock, D. W., D. L. Ellies, Z. Zhao, M. Ekker, F. H. Ruddle and K. M. Weiss (1996). "The evolution of the vertebrate Dlx gene family." Proc Natl Acad Sci U S A **93**(20): 10858-10863.

Takahashi, M. (2001). "The GDNF/RET signaling pathway and human diseases." Cytokine Growth Factor Rev **12**(4): 361-373.

Takahashi, M., J. Ritz and G. M. Cooper (1985). "Activation of a novel human transforming gene, ret, by DNA rearrangement." Cell **42**(2): 581-588.

Tam, P. K. and M. Garcia-Barcelo (2009). "Genetic basis of Hirschsprung's disease." Pediatr Surg Int **25**(7): 543-558.

Tian, H., B. Biehs, S. Warming, K. G. Leong, L. Rangell, O. D. Klein and F. J. de Sauvage (2011). "A reserve stem cell population in small intestine renders Lgr5-positive cells dispensable." Nature **478**(7368): 255-259.

Uesaka, T., S. Jain, S. Yonemura, Y. Uchiyama, J. Milbrandt and H. Enomoto (2007). "Conditional ablation of GFRalpha1 in postmigratory enteric neurons triggers unconventional neuronal death in the colon and causes a Hirschsprung's disease phenotype." Development **134**(11): 2171-2181.

Uesaka, T., M. Nagashimada, S. Yonemura and H. Enomoto (2008). "Diminished Ret expression compromises neuronal survival in the colon and causes intestinal aganglionosis in mice." J Clin Invest **118**(5): 1890-1898.

Uesaka, T., H. M. Young, V. Pachnis and H. Enomoto (2016). "Development of the intrinsic and extrinsic innervation of the gut." Dev Biol **417**(2): 158-167.

van der Flier, L. G. and H. Clevers (2009). "Stem cells, self-renewal, and differentiation in the intestinal epithelium." Annu Rev Physiol **71**: 241-260.

Wu, J. J., J. X. Chen, T. P. Rothman and M. D. Gershon (1999). "Inhibition of in vitro enteric neuronal development by endothelin-3: mediation by endothelin B receptors." Development **126**(6): 1161-1173.

Yan, K. S., L. A. Chia, X. Li, A. Ootani, J. Su, J. Y. Lee, N. Su, Y. Luo, S. C. Heilshorn, M. R. Amieva, E. Sangiorgi, M. R. Capecchi and C. J. Kuo (2012). "The intestinal stem cell markers Bmi1 and Lgr5 identify two functionally distinct populations." Proc Natl Acad Sci U S A **109**(2): 466-471.

Yu, M., T. Mazor, H. Huang, H. T. Huang, K. L. Kathrein, A. J. Woo, C. R. Chouinard, A. Labadorf, T. E. Akie, T. B. Moran, H. Xie, S. Zacharek, I. Taniuchi, R. G. Roeder, C. F. Kim, L. I. Zon, E. Fraenkel and A. B. Cantor (2012). "Direct recruitment of polycomb repressive complex 1 to chromatin by core binding transcription factors." Mol Cell **45**(3): 330-343.

Zhang, H., G. Hu, H. Wang, P. Sciavolino, N. Iler, M. M. Shen and C. Abate-Shen (1997). "Heterodimerization of Msx and Dlx homeoproteins results in functional antagonism." Mol Cell Biol **17**(5): 2920-2932.

Zhang, Q., J. Zagozewski, S. Cheng, R. Dixit, S. Zhang, J. de Melo, X. Mu, W. H. Klein, N. L. Brown, J. T. Wigle, C. Schuurmans and D. D. Eisenstat (2017). "Regulation of Brn3b by Dlx1 and Dlx2 is required for retinal ganglion cell differentiation in the vertebrate retina." Development.

Zhang, Z. and J. Huang (2013). "Intestinal stem cells - types and markers." Cell Biol Int **37**(5): 406-414.

Zhou, Q. P., T. N. Le, X. Qiu, V. Spencer, J. de Melo, G. Du, M. Plews, M. Fonseca, J. M. Sun, J. R. Davie and D. D. Eisenstat (2004). "Identification of a direct Dlx homeodomain target in the developing mouse forebrain and retina by optimization of chromatin immunoprecipitation." Nucleic Acids Res **32**(3): 884-892.

Zorn, A. M. and J. M. Wells (2009). "Vertebrate endoderm development and organ formation." Annu Rev Cell Dev Biol **25**: 221-251.